Stable Isotope Thermometry at High Temperatures

Article *in* Reviews in Mineralogy and Geochemistry · January 2001

DOI: 10.2138/gsrmg.43.1.365

CITATIONS
148

READS
556

1 author:

J. W. Valley
University of Wisconsin–Madison
779 PUBLICATIONS **31,015** CITATIONS

SEE PROFILE

6 Stable Isotope Thermometry at High Temperatures

John W. Valley

Department of Geology & Geophysics
University of Wisconsin
1215 West Dayton Street
Madison, Wisconsin 53706

INTRODUCTION

Determination of accurate temperatures for geological events has been the grail of stable isotope geochemistry since the seminal 1947 paper by Urey. In theory, this should be simple. Calibrated mineral pairs are common, analysis is rapid, and there is no significant pressure correction. However, in spite of widespread application, the promise of reliable thermometry has been elusive. Stable isotope temperatures in metamorphic and igneous rocks are often controversial; is the fractionation between two phases a thermometer, speedometer (rate dependant), hygrometer ($P(H_2O)$-dependant), or chimera? A number of factors have contributed to this uncertainty including: incomplete and sometimes conflicting calibration of isotope fractionation factors; limited understanding of the kinetics of mineral exchange; and the lack of microanalytical techniques. This situation has improved dramatically over the past decade, permitting reliable and detailed thermal histories to be inferred.

In a landmark paper, Bottinga and Javoy (1975) empirically calibrated the oxygen isotope fractionation factors among ten rock-forming minerals at T > 500°C. Their compilation shows that 84% of analyzed samples contain at least three minerals meeting a concordance test for equilibrium. They concluded "the great majority of igneous and metamorphic rocks …. has conserved a state of oxygen isotope exchange equilibrium." If correct, this bodes well for thermometry. However, this conclusion was contested by Deines (1977) who critically examined the existing data and concluded that "less than half of the rocks analyzed to date would yield concordant ^{18}O-derived temperatures." While seeming irreconcilable, both conclusions are based on fact. All rocks contain some degree of disequilibrium, but many also preserve a thermometric record. It is the purpose of this review to discuss the new strategies for reliable isotope thermometry and to explore disequilibrium processes so they may be recognized and properly interpreted.

The organization of this paper will be to discuss the assumptions of thermometry, processes of isotope exchange, and approaches for recovering temperature estimates of identifiable geological events. This is followed by applications of oxygen and carbon isotope thermometry to metamorphic and igneous rocks. While many careful studies have been published since 1947, emphasis will be placed on studies that have benefited from technical, experimental, and theoretical advances of the past decade.

REQUIREMENTS OF STABLE ISOTOPE THERMOMETRY

In theory, temperature can be estimated if minerals of interest record equilibrium conditions for a specific geologic event. Analysis of any two coexisting phases defines the isotope fractionation and uniquely determines the temperature of equilibration.

In practice, rocks follow a temperature-time path, equilibration is difficult to prove, and a number of conditions must be met for stable isotope thermometry to be accurate. The assumption that these conditions have been met is implicit in all thermometry, but

1529-6466/00/0043-0006$05.00

may not be fully evaluated. Similar requirements apply to petrologic geothermometry which is based on the partitioning of cations (see Essene 1989, Spear and Florence 1992).

There are three basic conditions for successful stable isotope thermometry.

(1) The sample domain was equilibrated in a specific event and compositions are "frozen-in". Thus, at the scale of measurement, minerals do not contain growth zonation or retrograde alteration.

(2) Analysis of isotope ratio is accurate at the appropriate scale.

(3) Isotope fractionation is sufficiently sensitive to temperature and is accurately calibrated, including the effects of solid solution, mixed fluids, and pressure.

Thus, the best stable isotope thermometers will have large fractionations, involve relatively common minerals, and occur in rocks where equilibration can be evaluated. The ideal case is a rock where all minerals crystallized at a specific temperature (diagenetic, metamorphic or igneous), and then cooled rapidly in a closed system. In other situations, knowledge of the exchange kinetics of the minerals in question can be important in the choice of thermometer.

If the first condition for thermometry (above) is not met, then stable isotope data contain information on interesting and more complex aspects of the thermal and fluid history. Rocks commonly preserve partial records of the varying conditions they have enjoyed: P-T-time-fluid-deformation. In well defined situations, multiple events can be identified or characterized in the evolution of a terrane, including: conditions during polymetamorphism; development of multiple fabrics; temperatures at specific reactions along the prograde or retrograde P-T path; sources of fluid infiltration during prograde, peak, or retrograde metamorphism; open or closed system recrystallization; crystallization of anatectic melts; assimilation during fractional crystallization of magmas; water fugacity during cooling; prograde heating rate; or cooling rate during uplift. The ability to study seemingly "invisible" retrograde history or to "see through" the peak of metamorphism is evolving rapidly. Such work will be discussed here as it applies to thermometry, but a full review is beyond the scope of this paper.

ANALYSIS OF STABLE ISOTOPE RATIOS

The first discoveries of stable isotope geochemistry were made possible by development of the Nier-type (gas-source, double-collecting) mass-spectrometer (Nier 1947), which improved analytical precision of light stable isotopes from ~2 ‰ to 0.05 ‰ (Murphey and Nier 1941, McCrea 1950). Modern gas-source mass-spectrometers are capable of measuring $\delta^{18}O$ to within a standard error of 0.003 ‰ (3 per meg, Luz et al. 1999). The analytical accuracy associated with thermometry is limited by sample preparation, not mass-spectrometry.

Table 1 summarizes the capabilities of laser and ion microprobe analysis in comparison to the time-honored conventional techniques. Figure 1 shows the advantages and trade-offs involved in the newer techniques: spatial resolution vs. accuracy and precision vs. cost of analysis. These factors will be discussed further under 'Microanalysis.' Continuous flow mass-spectrometry (Merritt and Hayes 1994); IR-spectroscopy (Kerstel et al. 1999, Esler et al. 2000); large radius, multi-collector ion probes (McKeegan and Leshin, this volume); automation; and shorter wavelength UV lasers (Young et al. 1998, Farquhar and Rumble 1998, Fiebig et al. 1999, Jones et al. 1999) also hold promise for enhanced analytical capabilities and better thermometry.

Table 1. Characteristics of various techniques for light stable isotope analysis (Valley 1998).

Technique	Isotopes, Minerals	Sample Prep.	Typical Sample Size	Spatial Resolution		Precision (1 sd)	References
CONVENTIONAL TECHNIQUES							
Ni reaction vessels	O silicates, oxides	Powder or chips	10-20 mg		-	0.2‰[A]	1
Phosphoric acid	O,C carbonates	Powder or chips	> 10µg		-	0.03-0.1‰[B]	2
Combustion	C graphite, diamonds	Powder or chips	> 1µg		-	0.03‰	3
Combustion	S	Powder or chips	> 1 mg		-	0.1‰	4
Fusion	H solids	Powder or chips	50-100 mg		-	1-2‰	5
LASER PROBE / MASS-SPECTROMETER							
Laser probe, IR	O silicates, oxides	Powder or chips	≥ 0.5 mg	500	µm	0.07‰	6,7
Laser probe, IR	O silicates, oxides	In situ	≥ 0.5 mg	500	µm (5mm)[C]	0.3-0.5‰	6
Laser probe, IR	S	In situ, chips	≥0.1 mg	200	µm	0.2‰	8
Laser probe, IR	O,C carbonates	In situ	≥0.5 mg	500	µm	[D]	9
Laser probe, IR	O phosphates	Powder or chips	≥0.5 mg	500	µm	0.1‰	10
Laser probe, UV	O silicates, oxides	In situ	~ 0.5 mg	~500	µm	0.1‰	11
Laser probe, UV	O phosphates	In situ		300x400	µm	0.4‰	12
ION MICROPROBE / SIMS							
Ion probe	O oxides (conductors)	In situ	0.4 ng	8	µm	0.5-1‰	13
Ion probe	O silicates or conductors	In situ	5 ng	20	µm	0.5-1‰	14
Ion probe	O carbonates	In situ	5 ng	20	µm	0.5-1‰	15
Ion probe	S	In situ	1-5 ng	10-20	µm	0.25-1‰	16
Ion probe	H	In situ	5-10 ng	20-30	µm	10‰	17
Ion probe	C	In situ	1-5 ng	10-30	µm	0.5-1‰	18

Footnotes; [A]some labs analyze 2 mg and attain precision ≤0.1 per mil; [B]precision for C is typically better than for O; [C]in situ pits are surrounded by 5mm haloes that prevent high analysis density, and causes fractionation with IR lasers. UV lasers may prevent such edge effects for improved spatial resolution and precision (Weichert and Hoefs, 1995); [D]precision and accuracy may be sample and procedure dependent.

REFERENCES: 1. Clayton and Mayeda, 1963; 2. McCrea, 1950; Sharma and Clayton, 1965; Rosenbaum and Sheppard, 1986; 3. Craig, 1953; DesMarais and Moore, 1984; 4. SO_2: Rafter, 1957; Robinson and Kusakabe, 1975; SF_6: Rees, 1978; 5. Bigeleisen et al., 1952; Godfrey, 1962; 6. Sharp, 1990; Elsenheimer and Valley, 1992; 7. Valley et al., 1995; 8. Crowe et al., 1990; 9. Smalley et al., 1989; Sharp and Cerling, 1996; 10. Kohn et al., 1996; 11. Weichert and Hoefs 1995; Farquhar and Rumble 1998; Fiebig et al., 1999; 12. Jones et al., 1999; 13. Valley and Graham, 1991a; 14. Hervig et al., 1992; Eiler et al., 1997a; 15. Valley et al., 1998; 16, Deloule et al., 1986; Eldridge et al., 1988; Riciputi, 1996; 17. Deloule et al., 1991a,b; 18. Zinner et al., 1989; Harte and Otter, 1992; Eiler et al., 1997b.

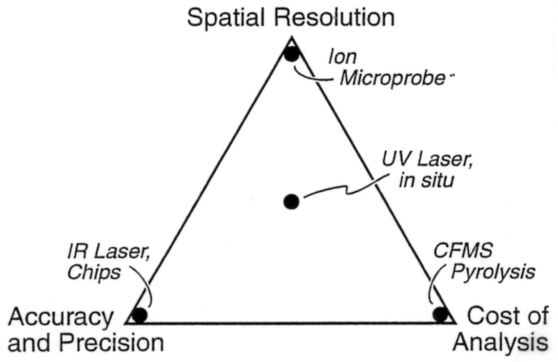

Figure 1. Advantages and trade-offs of new analytical techniques for stable isotope analysis (see Table 1). At present, the best accuracy and precision is achieved for $\delta^{18}O$ by IR-laser fluorination of chips or powdered samples; the fastest and least expensive analyses are made by automated pyrolysis systems with continuous flow mass-spectrometers (CFMS); and the smallest samples and best *in situ* spatial resolution is attained by ion microprobe. The capabilities of *in situ* UV-laser fluorination are intermediate.

Microanalytical techniques are increasingly useful for stable isotope thermometry. Analytical precision for $\delta^{18}O$ of 1 ‰ can be obtained from 0.3-0.4 ng samples (≅ 75 μm^3) by single collecting, small radius ion microprobe at high mass-resolution (Valley and Graham 1991, Valley et al. 1998a). Double collecting, large radius instruments offer enhanced counting efficiency and precision a factor of 2 better for similar spot sizes (McKeegan and Leshin, this volume). This is a dramatic improvement over the mg-size samples required before 1991. The question arises; how much smaller will be possible? The ultimate limit comes from counting statistics for a Gaussian distribution; 10^8 atoms of ^{18}O must be counted to obtain one standard deviation equal to 0.1 ‰. At natural abundances, this oxygen will be mixed with 5×10^{10} atoms of ^{16}O, the equivalent of

approximately 3×10^{-3} ng of mineral. Perfect efficiency will never be attained and spots smaller than 1 μm^3 are unlikely, though sub-micron linear resolution is possible today by depth profiling. This spatial resolution is competitive with that of elemental analysis by electron microprobe, and brings the length scales of oxygen diffusion for igneous and metamorphic processes within the reach of stable isotope analysis. It also opens the door for investigation of a wide range of thin overgrowths and small particles of interest to sedimentary, environmental, or biological studies.

CALIBRATION OF ISOTOPE FRACTIONATION

The theory of stable isotope exchange was described by Urey (1947) and Bigeleisen and Mayer (1947), and has been reviewed and elaborated many times (Javoy 1977, Clayton 1981, O'Neil 1986, Hoefs 1997, Criss 1999; Chacko et al., this volume; Cole and Chakraborty, this volume). Only the basic equations need be given here.

For any two minerals in isotopic equilibrium, an exchange reaction relates the isotopic end-member compositions. This is illustrated by the exchange of oxygen isotopes between quartz and rutile (Reaction 1). The example is simplified by writing the mineral formulae with one oxygen, but the approach is general for SiO_2-TiO_2, or any mineral pair containing an element of interest.

$$Ti_{0.5}{}^{18}O + Si_{0.5}{}^{16}O = Ti_{0.5}{}^{16}O + Si_{0.5}{}^{18}O \quad (1)$$

The equilibrium constant for Reaction (1) is also the fractionation factor:

$$K_{eq} = \left[\frac{\left(^{18}O/^{16}O\right)\text{quartz}}{\left(^{18}O/^{16}O\right)\text{rutile}} \right] = \alpha\,^{18}O\,(Qt - Rt) \quad (2)$$

$$1000 \left(\frac{-\Delta G^{o}}{RT} \right) = 1000 \ln K_{eq} = 1000 \ln \alpha\,(Qt - Rt) \cong \Delta\,^{18}O\,(Qt - Rt) \quad (3)$$

Thus, fractionation is mostly dependent on temperature. Since isotopes differ only in their nucleus, the volume change of Reaction (1) is very small. From the relation $\delta G = -S\delta T + V\delta P$, it follows that there is generally little or no measurable effect of pressure on fractionation (Clayton et al. 1975, Polyakov and Kharlashima 1994; Chacko et al., this volume).

The principle means of calibrating mineral thermometers are experiment, theoretical calculation, the increment method, and empirical comparison with other thermometers. It is common practice to assume linearity of 1000 ln α vs. T^{-2} according to the relation:

$$1000 \ln \alpha(a\text{-}b) = A_{a\text{-}b} \times 10^6 / T^2 \quad (4)$$

Most mineral systems can be approximated by Equation (4). However, for fluids it has been shown theoretically (Stern et al. 1968) and experimentally (see Friedman and O'Neil 1977) that cross-overs and other complex behavior can occur and thus higher order polynomials are sometimes fit to fractionation data. When available, high pressure, solid-solid exchange experiments are most generally reliable (see Clayton and Kieffer 1991, Matthews 1994, Rosenbaum and Mattey 1995). Figure 2 shows experimentally determined fractionations for calcite vs. some common rock-forming minerals (Clayton and Kieffer 1991). Experimental calibrations involving aqueous fluids are not fully understood and may depend on additional factors including solutes, fluid speciation, mixed data for vapor and supercritical fluid, recrystallization, and pressure (Clayton et al. 1989, Matthews 1994). Increment method calculations are a useful first approximation,

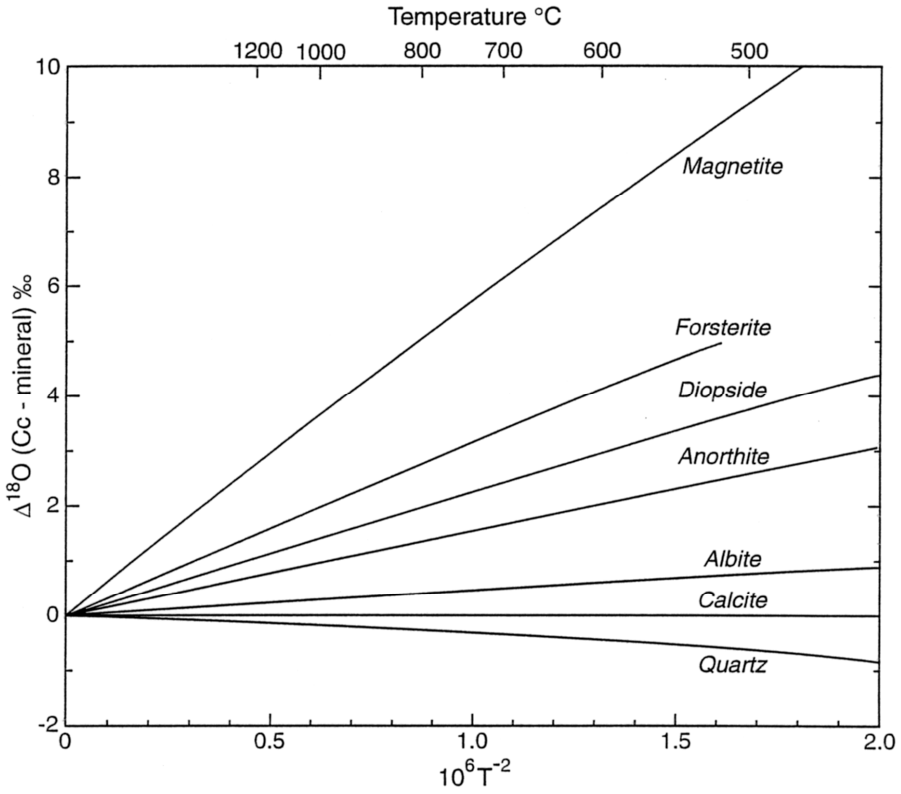

Figure 2. Experimentally determined oxygen isotope fractionations between calcite and quartz, albite, anorthite, diopside, forsterite and magnetite (Clayton and Kieffer 1991).

but should be independently evaluated. This subject is reviewed by Chacko, Cole and Horita (this volume) and only empirical calibrations, which depend on independent thermometry (e.g. petrologic estimates of T), will be discussed in detail below.

A useful Excel spreadsheet compiles published calibrations (uncritically) for easy calculation (J.D. Martin, unpublished) as does a web site (http://www.ggl.ulaval.ca/cgi-bin/isotope/generisotope.cgi) by Beaudoin and Therrien. The critical evaluation of various calibrations of equilibrium fractionation is essential to accurate thermometry. This topic is discussed in detail by Chacko, Cole and Horita (this volume).

KINETICS OF MINERAL EXCHANGE

Apparent temperature

The measurement of isotope fractionation between two equilibrated phases yields one estimate of temperature, and n phases yield (n – 1) temperatures. In the real world where equilibrium may be imperfectly attained, recorded, or preserved, analysis of n minerals provides at least (n – 1) estimates of apparent temperature (T_A) and often many more. These values of T_A may represent the true temperature of a meaningful geologic event or they may be spurious. The choices of both the appropriate strategy of analysis and the correct interpretation will depend on the history of the rock.

Post-crystallization exchange can take many forms that will complicate thermometry. Figure 3 shows four cartoons of the isotope distribution predicted for various processes of hydrothermal alteration of quartz by a low $\delta^{18}O$ fluid. If diffusion is radial and inward from the grain boundary then a concentric zonation of $\delta^{18}O$ is predicted with a smooth error function shaped gradient (Fig. 3A and Fig. 4). If the rim of the crystal

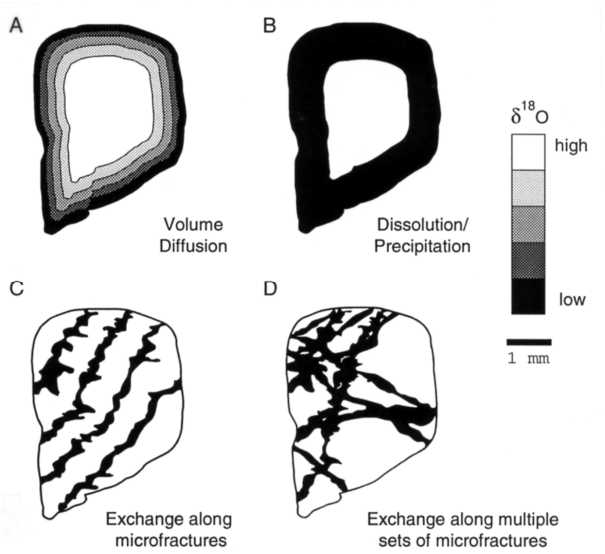

Figure 3. Schematic representation of the oxygen isotope zonation developed in a mineral by exchange with low $\delta^{18}O$ fluids through different mechanisms: (A) volume diffusion inward from the grain boundary; (B) dissolution and reprecipitation; (C) exchange along a set of microfractures; and (D) exchange along multiple sets of microfractures. Distinguishing among these processes requires microanalysis (Elsenheimer and Valley 1992).

is recrystallized to form an overgrowth then the concentric pattern should have a steep gradient against the core of the crystal, i.e. a step function partially smoothed by any diffusional exchange (Fig. 3B). If micro fractures cause recrystallization within the crystal, then more complex patterns of heterogeneity are possible combining recrystallization and diffusion (Figs. 3C and 3D). Some amount of diffusion is inescapable in all samples and the magnitude of diffusive exchange must always be considered, although it may be insignificant at the scale of observation in some cases.

Diffusion

Diffusion is a significant and predictable process of intercrystalline (and intracrystalline) isotope exchange. Discussion will concentrate on self-diffusion involving exchange of isotopes of major elements such as oxygen, which is distinct from chemical diffusion or tracer diffusion (Lasaga 1998). The Arrhenius equation

$$D = D_o e^{-E/RT} \quad (5)$$

relates D (diffusion coefficient, cm^2/s or m^2/s), D_o (pre-exponential factor, cm^2/s or m^2/s), E (activation energy, sometimes represented as Q, J/mol), R (gas constant, 8.3143J/°K·mol), and T (temperature, K). The use of different units, especially in earlier literature, can be confusing.

Diffusion rates are highly variable. Volume diffusion through the crystal lattice is often the rate-limiting step in inter-mineral exchange. The extent of exchange by volume diffusion depends on the phases present, the nature of the grain boundary, diffusion coefficients, activation energies, crystal size (or diffusion distance), and thermal history. Large differences in D exist from mineral to mineral (see review by Cole and Chakraborty, this volume). Diffusion rates of oxygen correlate with ionic porosity for many anhydrous minerals (Fortier and Giletti 1989, Zheng and Fu 1998) such that less dense tectosilicates like feldspar and quartz have faster diffusion than more densely packed ino- or orthosilicates like pyroxene or olivine. Thus, in a dry rock, diffusion is retarded by increasing pressure which tends to reduce ionic porosity, but the effect of increased $P(H_2O)$ or $f(H_2O)$ is to speed diffusion. Volume diffusion can also be strongly dependent on mineral chemistry. Diffusion rates may also be highly anisotropic, and experimental calibrations of anisotropy are needed for many minerals.

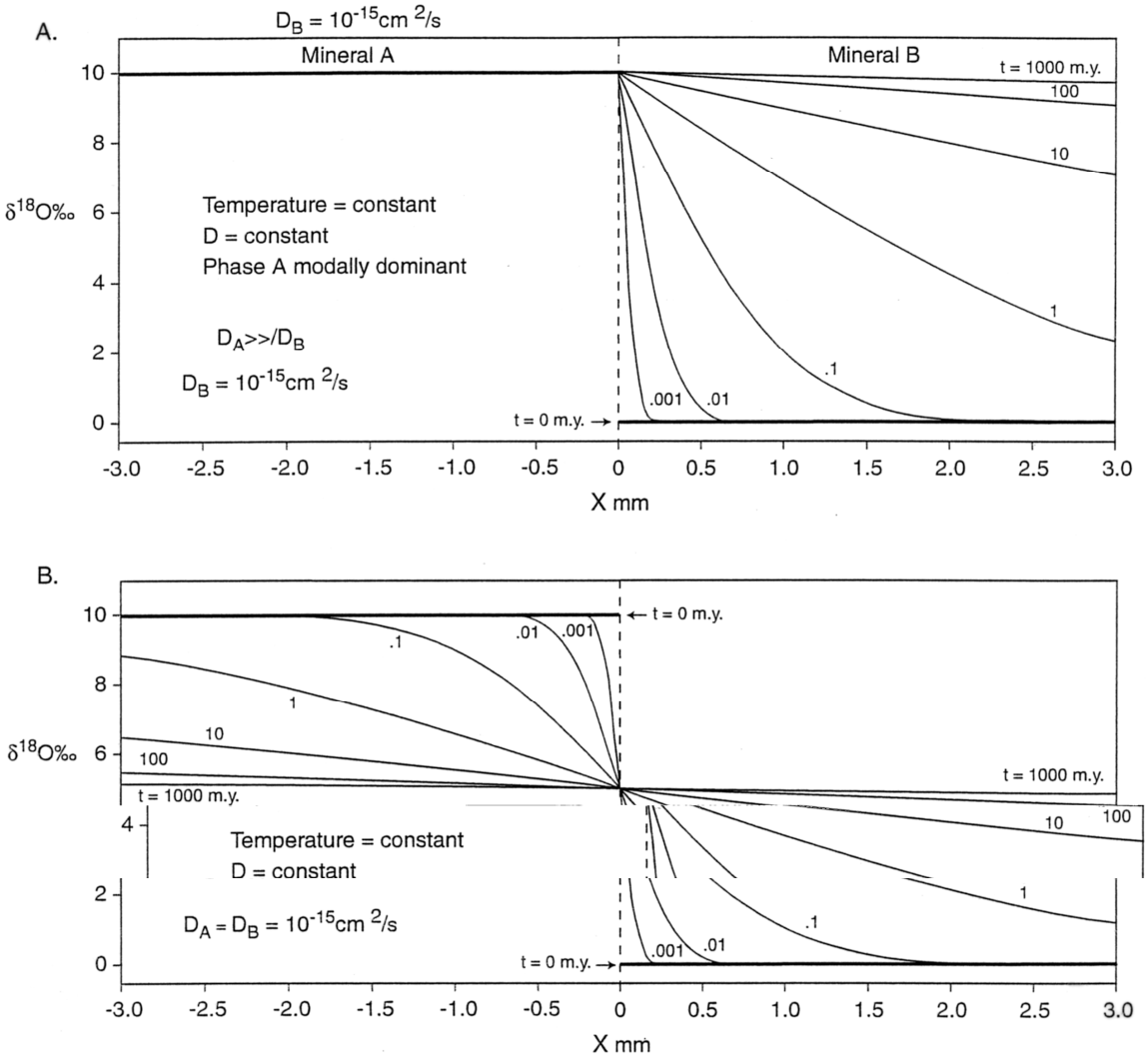

Figure 4. One-dimension diffusion profiles across the boundary of two touching minerals at constant temperature and variable times. Calculations assume an initial step in $\delta^{18}O$ of 10 ‰ and a final equilibrium fractionation of Δ(A-B) = 0 ‰. (A) Pinned boundary condition where Mineral A is modally dominant and has fast oxygen diffusion such that its $\delta^{18}O$ does not vary during exchange. (B) a diffusion couple where the abundance and diffusion properties are the same in both minerals, and Δ(A-B) = 0 ‰.

In contrast to volume diffusion through a crystal lattice, diffusion through a fluid, along a grain boundary, or on a surface is more rapid (Fig. 5). Thus, grain boundaries will be significant pathways for exchange, especially if they are hydrated, discordant, or filled with hydrous alteration or fluid. Even apparently anhydrous grain boundaries between unlike minerals in granulite facies gneisses are zones of high ionic porosity and promote intercrystalline exchange (Eiler et al. 1995a). Diffusion rates along dry coherent crystal boundaries may be significantly slower, close to volume diffusion. Thus some exsolution lamellae will create fast pathways for diffusive exchange (Nagy and Giletti 1986, Farquhar and Chacko 1994) while others are not measurably different (Schwarcz 1966).

Effect of deformation

Isotope exchange is enhanced by deformation (Kerrich et al. 1977, Farquhar et al.

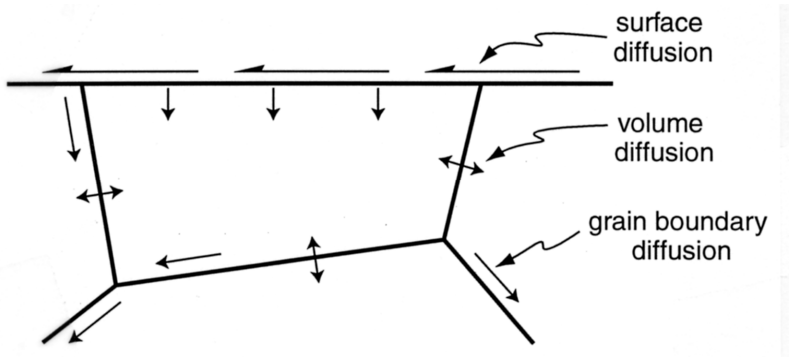

Figure 5. Pathways for diffusion. The relative diffusion rates decrease: surface > grain boundary > volume diffusion. In many rocks, diffusion and exchange is so much faster along grain boundaries than through the crystal lattice that grain boundaries can be modeled as equilibrated at temperatures where intermineral exchange is important.

1996). Commonly deformation is accompanied by recrystallization and minerals will readily exchange with fluids or other exchangeable phases, but volume diffusion rates will be enhanced by any process that facilitates breaking of oxygen-cation bonds. Mylonites are often shifted in $\delta^{18}O$ relative to their protolith (Cartwright et al. 1993). Farver and Yund (1999) experimentally studied bulk oxygen exchange in a natural sample of mylonite. Combined TEM and ion microprobe analysis showed faster oxygen diffusion parallel to the foliation of this very fine grained (~5 μm), micaceous (15-20% biotite) sample, consistent with fast pathways of exchange via a thin interconnected aqueous film along grain boundaries. These results also indicate that oxygen transport is several orders of magnitude faster through micaceous lithologies than in experiments of mono-mineralic quartzites or marbles (Farver and Yund 1991a, 1992, 1995a,b; 1998).

The fine grain size and differing mechanisms of exchange complicate thermometry in highly deformed rocks. O'Hara et al. (1997) correlate oxygen exchange with quartz and feldspar textures. Heterogeneous strain is associated with partial exchange while homogeneous strain correlates to isotopic homogenization on a grain scale. Reasonable, self-consistent temperatures have been estimated in favorable cases for deformation (350-400°C, O'Hara et al. 1997) and for retrograde fluid infiltration of granulites (600°C, Hoernes et al. 1995). Morrison and Anderson (1998) found that quartz-epidote fractionations increase approaching (50 to 12 m) the detachment fault of the Whipple mountains metamorphic core complex due to cooling by circulating surface-derived fluids.

Effect of water fugacity

Many minerals have been shown to experience oxygen diffusion that is several orders of magnitude faster in hydrothermal vs. anhydrous experiments (see Cole and Chakraborty, this volume). The exact causes of this relation are controversial: do protons diffuse rapidly through the crystal hydrating bonds, is H_2O the diffusing species, is the effect of $f(H_2O)$ inherited via charge-balanced substitutions from the time of crystallization or does diffusion rate (D) adjust rapidly to changing fluid environments, and does D scale linearly with $f(H_2O)$ (Giletti and Yund 1984, Elphick and Graham 1988, Farver and Yund 1991b, Zhang et al. 1991, McConnell 1995, Doremus 1998, Zheng and Fu 1998). Grain boundary diffusion rates are also enhanced by the presence of aqueous fluid (Farver and Yund 1992).

The scale of isotope equilibration and the magnitude of diffusive retrogression is critically dependent on the fluid conditions of a rock. Dry, granulite facies metamorphism has been invoked to explain very slow diffusion and the preservation of high oxygen isotope temperatures in some rocks (Sharp et al. 1988, Farquhar et al. 1996) while variable $f(H_2O)$ during cooling has explained faster diffusion and resetting of $\delta^{18}O$ in diopsides from granulite facies marbles (Edwards and Valley 1998), and of amphibolites and pelites (Kohn 1999). The rapid decrease in water activity that is common during closed-system cooling after the peak of metamorphism will cause chemical quenching in rocks that are water saturated during prograde metamorphic dehydration and anhydrous during cooling.

DIFFUSION MODELS

Diffusion distance

Figure 4A shows the $\delta^{18}O$ profile developed after isothermal diffusion for varying lengths of time based on the relation:

$$C = C_o \operatorname{erfc}\left(\frac{X}{2\sqrt{Dt}}\right) \tag{6}$$

where C_o, the composition of mineral A, is held constant; C, the composition at distance X in mineral B, is initially zero; D is the diffusion constant, t is time, and erfc is the inverse error function (Crank 1975, Eqn. 2.45). This equation and (3.13) assume one-dimensional diffusion in a semi-infinite medium. Equations (6.18) to (6.20) in Crank (1975) model spherical geometry. For oxygen isotopes, $\delta^{18}O$ can be substituted for composition or isotope ratio. In Figure 4, D is set at 10^{-15} cm^2/s in mineral B (a mid-range for many igneous and metamorphic minerals at mid-crustal temperatures) and in 4A the profile is "pinned" by assuming $D_A \gg D_B$ so the composition remains constant at the grain boundary. It is assumed that $\Delta(A\text{-}B) = 0$ and that the mass of A is infinite, i.e. large enough to maintain a constant composition after exchange. These last two conditions would also be met if the grain boundary transport is fast, or if phase A is a fluid that is abundant in comparison to the exchanged volume of B. Calculations with Equation (6) are aided by the useful approximation:

$$\operatorname{erf}(a) = \sqrt{1 - e^{-(4a^2/\pi)}} \tag{7}$$

where erfc a = 1 – erf a (Lasaga 1998). From Figure 4A, it is seen that an initial step profile decays into a migrating diffusion profile.

It is often useful to refer to "diffusion distance" in order to approximate the magnitude of diffusive exchange for given Dt, but Figure 4A shows that there is no unique distance unless the percentage of exchange is defined. The simplest diffusion distance is defined for 50% exchange, i.e. the distance X to the point in mineral B where 50% of the initial difference has exchanged ($C/C_o = 0.5$, $\delta^{18}O = 5$ ‰); then Equation (6) reduces to:

$$X = \sqrt{Dt} \tag{8}$$

Figure 4B shows the diffusion profiles that will develop in semi-infinite sheets from the same initial step of 10‰ if $D_A = D_B = 10^{-15}$ cm^2/s and $\Delta(A\text{-}B) = 0$.

Dodson's closure temperature

The concept of closure or blocking temperature (T_C) below which exchange

effectively ceases has been applied to both stable and radiogenic isotopes, and to cations. While many processes can contribute to exchange, the most successful treatments of T_C have been in systems that are dominated by volume diffusion into a crystal from its grain boundary.

The Dodson equation (Eqn. 9) defines T_C strictly in terms of diffusion. Use of T_C (Eqn. 9) implicitly assumes that other processes are not important. The strong dependence of diffusion coefficient on temperature (Eqn. 5) causes the transition from rapid to slow diffusion during cooling to be over a relatively small temperature interval. Dodson (1973, 1979) presented an equation for the closure temperature, T_C of a single mineral:

$$T_c = \left\{ \frac{E/R}{\ln\left(\frac{-A\,R\,T_c^2\,(D_o/a^2)}{E\,(\delta T/\delta t)} \right)} \right\} \tag{9}$$

where A = diffusional anisotropy parameter, a = radius of mineral grain, and $\delta T/\delta t$ = linear cooling rate (see Appendix 1 in Giletti 1986). Thus closure temperatures are higher for lower values of diffusion coefficient (D in Eqn. 5), larger grain size, or faster cooling. Figure 6 shows values of T_C for oxygen in magnetite with variable radii from 1 to 0.01 mm and cooling rates from 1 to 1000°C/m.y. (Giletti and Hess 1988).

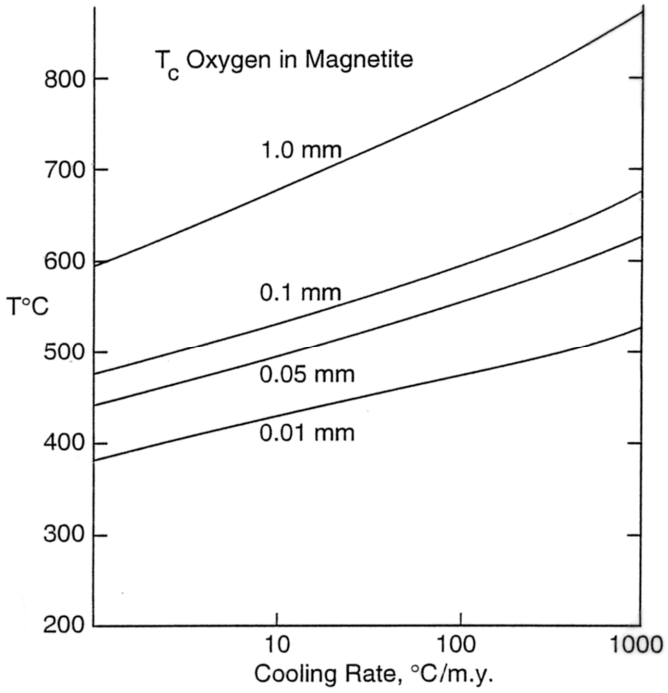

Figure 6. Calculated values of closure temperature for oxygen diffusion in magnetite of 1 to 0.01 mm in radius at cooling rates of 1 to 1000°C/m.y. (Giletti and Hess 1988).

Closure temperature is a useful concept for comparing the relative diffusivities of different minerals, or of the same mineral in different situations, but its applicability is limited by certain assumptions (Dodson 1973, Giletti 1986, Eiler et al. 1992, 1993). Dodson (1973) defined T_C for a radiogenic system as the temperature at the time corresponding to a mineral's apparent age, but its meaning may be somewhat different for oxygen isotopes. Equation (9) contains terms for the diffusion characteristics of only one mineral. It is implicit that this mineral is surrounded by an infinite, well-mixed reservoir of the element of interest. For many radiogenic systems, the loss of a trace element (e.g. Ar, Pb) is complete once it reaches a grain boundary and this condition is

met. However, for major elements, the grain boundary in not a large reservoir and a mineral can only change in composition if there is another phase with which to exchange. Thus, the properties of other minerals or fluids in a rock influence the actual closure of diffusive exchange. Furthermore, the transition to closure is not a single temperature; diffusion slows, but does not stop at any geologic temperature (Eqn. 5). Values of T_C are calculated for oxygen and carbon diffusion in selected minerals of thermometric interest under representative conditions in Table 3 (below).

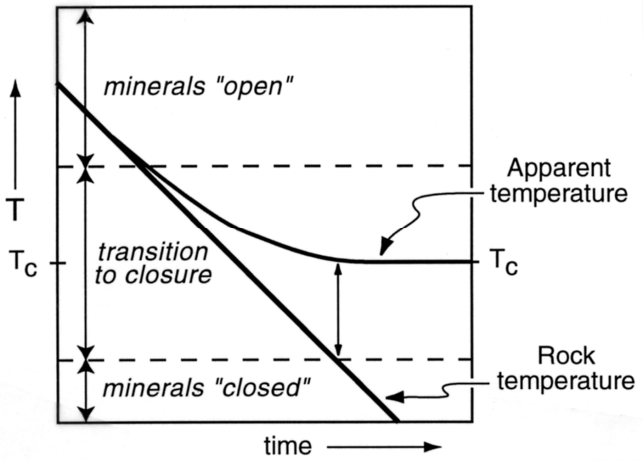

Figure 7. Plot of temperature vs. time during slow cooling. At high temperatures, minerals are "open" to exchange and the actual rock temperature (T_R) is equal to the apparent temperature (T_A) that would be estimated for the measured isotope fractionation between two minerals at that time. At intermediate temperatures, during the transition to closure: diffusion becomes slower; exchange is no longer able to keep up with increasing equilibrium fractionation; and T_A lags behind and is higher than T_R. At the end of the transition, minerals are closed, and T_A undergoes no further change and equals T_C. Note that the rock passes through T_C at an earlier time than T_A records T_C.

Figure 7 shows the apparent temperatures recorded by a mineral pair vs. the actual cooling path of a rock. As temperature approaches T_C, diffusion slows, exchange no longer keeps pace with declining temperature, and T_A diverges from actual rock T to asymptotically approach T_C. It is significant that closure occurs as a transition and not at a distinct temperature; once diffusion slows to the point where it retards exchange, the actual T of the rock becomes increasingly lower than apparent temperature or T_C. The time at which the rock finally records an apparent temperature equal to T_C is much later (and at lower T) than the time that the rock cooled through this temperature. Furthermore, diffusive exchange continues well below T_C near grain boundaries and will create isotopic profiles. Thus, T_C is an approximation for the transition to closure. These considerations are significant for interpretation of radiogenic as well as stable isotopes; the significance for stable isotope exchange will be discussed below.

The Giletti model

The first systematic treatment of stable isotope exchange by diffusion was applied to slowly cooled igneous and metamorphic rocks. Giletti (1986) used the Dodson closure temperature and hydrothermal experimental data for diffusion rates to calculate when minerals would cease exchanging with the rock during cooling. The computer program, COOL, can be used to make these calculations (Jenkin et al. 1991a,b). This is schematically represented in Figure 8 for a granite comprised of quartz, feldspar and hornblende. The relative values for equilibrium $\delta^{18}O$ decrease, Qt > Fsp > Hb, and the diffusion coefficients decrease Fsp > Qt > Hb. Thus hornblende has the lowest value of $\delta^{18}O$ and the slowest diffusion rate. The vertical dashed lines separating Periods I and II, and II and III are T_C for hornblende and quartz respectively at defined crystal size and cooling rate. At the initial temperature of 750°C, $\delta^{18}O$ values are equilibrated among minerals, representing magmatic crystallization or the thermal peak of metamorphism, and fractionations are small. During cooling through Period I, all minerals are open to diffusive exchange and reequilibration is continuous such that fractionations all increase

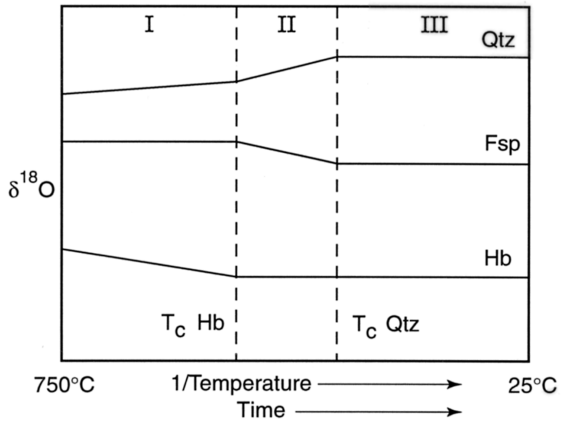

Figure 8. Schematic representation of $\delta^{18}O$ of quartz, feldspar and hornblende in an idealized granite undergoing diffusive exchange while cooling as described by the model of Giletti (1986). At high temperatures, above T_C(Hb), all three minerals are open to exchange and maintain equilibrium (Period I). At lower temperatures (Period II) hornblende is "closed" to oxygen diffusion and only quartz and feldspar continue to equilibrate. In this period, Δ(Fs-Hb) decreases although no feldspar-hornblende exchange occurs. Finally, below T_c(Qt), no further exchange can take place (Period III) and final fractionations are preserved (from Eiler et al. 1992).

with 1/T. During Period II, hornblende is closed and does not change in $\delta^{18}O$, but quartz and feldspar continue to exchange with one another. During Period III, only feldspar is still open to exchange and since exchange requires at least two phases, $\delta^{18}O$(Fsp) does not change.

Figure 8 illustrates important predictions of the Giletti model:

(1) None of the measured fractionations or T_A's record the formation temperature of the rock and are useful for thermometry, in the classical sense. This results because all minerals formed above their T_C.

(2) Only the fractionation between the two minerals with fastest diffusion in the rock (Qt-Fsp) has geologic significance. It records the closure temperature of the second fastest mineral, quartz, [i.e. T_A(Qt-Fsp) = T_C(Qt)].

(3) The final Δ(Fsp-Hb) is established at the end of Period II after hornblende has closed. This fractionation does not correspond to a temperature of equilibration or closure and, in the case presented by Figure 8; the apparent temperature is higher than any temperature experienced by the rock.

Other more general conclusions derive from the Giletti model.

(1) Reliable thermometry is possible if at least one mineral has formed below its closure temperature and other conditions are met.

(2) In minerals reset by diffusion, the apparent temperatures will be a function of grain size and mode in the rock, water activity that affects D, and thermal history.

(3) Cooling rates can be estimated in well-defined situations.

An important limitation of the Giletti model results from its reliance on the Dodson equation (Eqn. 9). This equation only considers one mineral in a rock and for major elements such as oxygen, a significant violation of mass balance can result.

The Fast Grain Boundary diffusion model (FGB)

The FGB model calculates exchange by diffusion of all minerals in a rock during cooling or heating (Eiler et al. 1992, 1993). This model considers any number of minerals and grain sizes in a rock, the diffusion characteristics of each mineral, the isotope fractionations, and various forms of $\delta T/\delta t$. It can be calculated with the computer program FGB (Eiler et al. 1994).

The main simplifying assumption of the FGB model is that all grain boundaries maintain isotopic equilibrium while the interior of each grain exchanges with its edge

according to the diffusional properties of that grain. This is a good approximation for oxygen exchange in many rocks because the grain boundary region is oxygen-rich and diffusion is many orders of magnitude faster than volume diffusion. In practice for most rocks, this criterion is only important over distances of about three grain diameters and must be maintained only at temperatures above T_C for the fastest diffusing minerals involved (samples from within diffusive exchange distance of rock contacts may be more complex). Eiler et al. (1995a) tested the assumption of fast grain boundary diffusion in an anhydrous granulite facies rock with coarse mineral banding and found that grain boundary exchange of oxygen was very rapid over distances of several centimeters. Thus, even in a worst-case scenario, the FGB assumption was upheld. The assumption should also apply in greenschist or amphibolite facies rocks where grain size is smaller and water activities higher, or in igneous rocks where temperature is higher.

The FGB model has significant advantages over the Giletti model which is limited by reliance on Dodson's closure temperature. FGB calculations can evaluate the importance of variable mineral mode, intracrystalline diffusion profiles, variable grain size, fluid infiltration, thermometry, and cooling rate for the interaction of all minerals in a rock (Eiler et al. 1992, 1993, 1995a,b). FGB calculations can also be used to predict which mineral systems and thermal conditions are most appropriate for accurate thermometry (Eiler et al. 1993, Ghent and Valley 1998, Putlitz et al. 2001), empirical estimation of isotope fractionations (Kohn and Valley 1998, King et al. 2001) or diffusion coefficients (Edwards and Valley 1998, Peck 2000), or cooling rate.

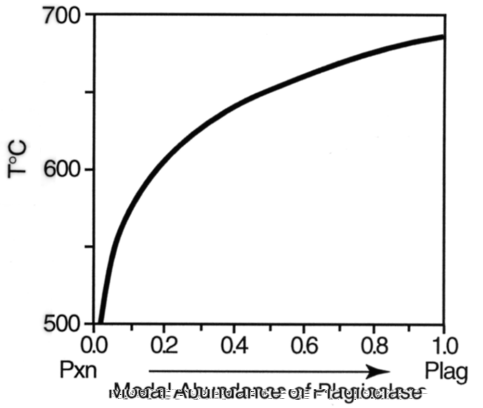

Figure 9. Plot of apparent temperature recorded between a mineral with slow oxygen diffusion (pyroxene) and a mineral with fast diffusion (plagioclase) vs. the modal percentage of plagioclase in a bi-mineral rock. Cooling is at 5°C/m.y. after peak equilibration at 750°C. In feldspar dominated rocks, T_A may preserve peak temperature, but for a rock dominated by pyroxene, T_A can be hundreds of degrees below peak T approaching 250°C, T_C(plag). The mode effect is modeled by the Fast Grain Boundary diffusion model and predicts that refractory accessory mineral (RAM) thermometers are most reliable (from Eiler et al. 1993).

The mode effect

A surprising and significant prediction of FGB calculations is that apparent temperature (T_A) is strongly dependent on mineral proportions. This is shown in Figure 9 where mineral mode is plotted against the T_A predicted by FGB for a simplified, two-mineral system: pyroxene-plagioclase, cooling (5°C/m.y.) after equilibration at 750°C. Plagioclase, the mineral with faster oxygen diffusion is plotted on the right and good agreement is predicted between T_C(Px) and T_A for a rock of this composition (anorthosite). This agreement arises because the rock is dominated by the faster mineral which acts as the well-mixed, infinite reservoir envisioned by Dodson (1973). Thus Δ(Plg-Pxn) thermometry is predicted to work in anorthosites if initial T is less than T_C(Pxn). However, a significant difference emerges as the proportion increases of pyroxene, the mineral with slower oxygen diffusion. For a pyroxene-rich rock, it is predicted that T_A will approach T_C(Plag). This difference arises because T_C (Eqn. 9) considers the diffusional characteristics of only one mineral. Thus, the Giletti approach ignores diffusion over short distances near the boundary of the slower mineral and incorrectly assumes that no further exchange is possible once the mineral with faster

diffusion cools below T_C of the second slowest mineral. In many rocks, the exchangeable, grain boundary regions of refractory minerals are a small reservoir and T_C (Eqn. 9) ≅ T_C (FGB). However, due to grain boundary diffusion, a significantly larger difference is predicted between T_C and T_A for the mineral proportions represented on the left side of Figure 9. In the case of a pyroxenite with traces of feldspar, the difference can be over 200°C. In this case, significant exchange will continue below T_C(Pxn) because the larger percentage of pyroxene rims is sufficient in mass to shift the $\delta^{18}O$ of the smaller amounts of plagioclase. This generalization leads to important predictions for thermometry as described for refractory accessory minerals.

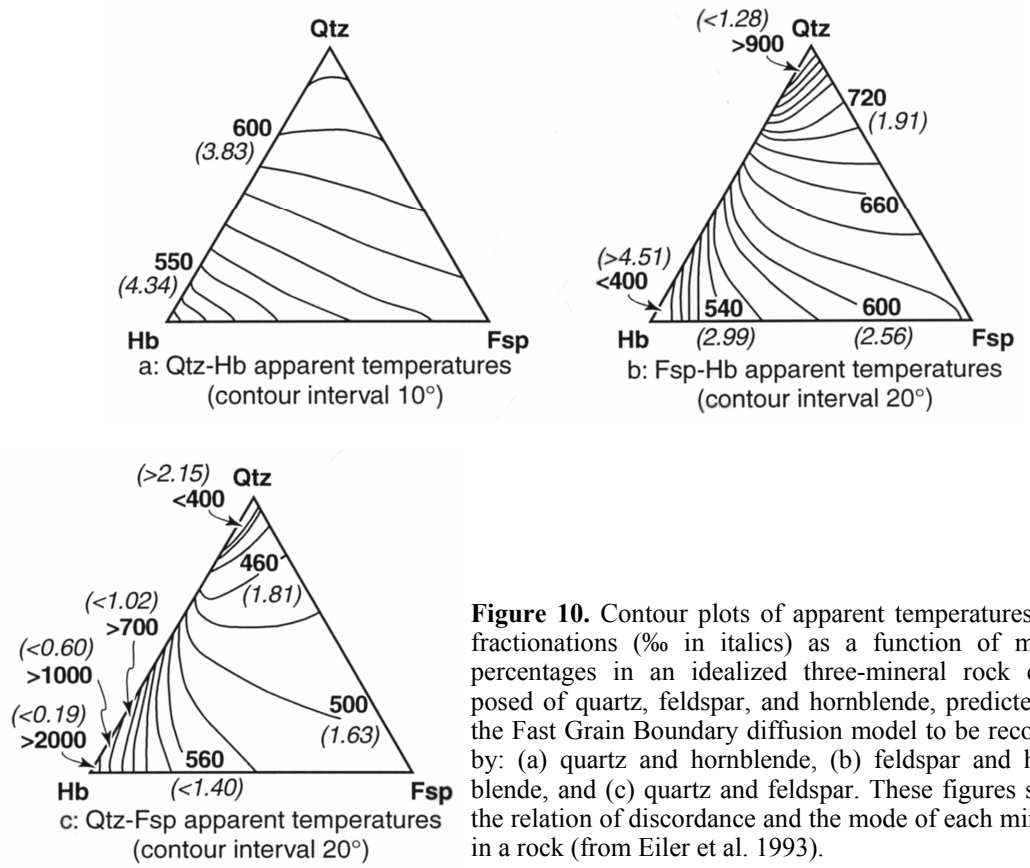

Figure 10. Contour plots of apparent temperatures and fractionations (‰ in italics) as a function of modal percentages in an idealized three-mineral rock composed of quartz, feldspar, and hornblende, predicted by the Fast Grain Boundary diffusion model to be recorded by: (a) quartz and hornblende, (b) feldspar and hornblende, and (c) quartz and feldspar. These figures show the relation of discordance and the mode of each mineral in a rock (from Eiler et al. 1993).

Mode effects can be complex for rocks composed of more than two minerals. This is shown in Figure 10, which predicts the apparent temperatures, recorded by Qtz-Hb, Fsp-Hb, and Qtz-Fsp pairs as a function of modal proportions in a three mineral rock that underwent slow cooling from 750°C. This figure illustrates some common problems of stable isotope thermometry in plutonic or high grade metamorphic rocks. Diffusion is relatively fast in each of these three minerals (i.e. T_C < 750°C) and the abundance of each mineral determines T_A. Peak temperatures will not be recorded, but erroneous apparent temperatures come fortuitously close to 750°C in a number of instances. While cooling rate can be estimated in a granite or other quartz-feldspar-hornblende rock, other minerals should be sought for reliable thermometry in this temperature range. Thus, T_C for each mineral and the mode effects for the rock can be used to predict which mineral systems will be accurate thermometers.

STRATEGIES FOR SUCCESSFUL THERMOMETRY

The theoretical models of inter-mineral and intra-mineral exchange provide a foundation for the interpretation of fractionation data for thermometry. However,

thermometry presents the inverse problem. In modeling, one assumes a temperature vs. time path and calculates the mineral compositions (and zonation) of the resulting rock. In thermometry, one is presented with measured compositions and must deduce the thermal history.

Isotope exchange trajectories

One approach to thermometry employs the whole rock $\delta^{18}O$, assuming no open system modification, as well as mineral data. The evolution of isotope ratio can be calculated for each mineral in the rock if inter-mineral equilibrium exchange is maintained during cooling at $T > T_C$ as shown in Figure 11. Farquhar et al. (1993) present equations for thermometry based on understanding the changing $\delta^{18}O$ for each mineral during cooling. They call this trend an Isotope Exchange Trajectory (IET) (Fig. 11). Calculation of IET's requires knowledge of the whole rock isotope ratio, and the modal abundance and fractionation factor for each mineral. For minerals in a single sample, this approach derives in part from that of Gregory and Criss (1986) and Gregory et al. (1987) who apply δ_i vs. δ_j diagrams to evaluate open and closed systems. Model temperatures calculated by the IET method will either be T_C for the highest T_C mineral or the peak T if one or more minerals formed at a temperature below its T_C. The precision of this approach is sensitive to the fractionation factor of the mineral with the highest T_C. Because all minerals must be accounted for, the accuracy of this approach depends on the complete absence of open system alteration, a requirement not made by other techniques.

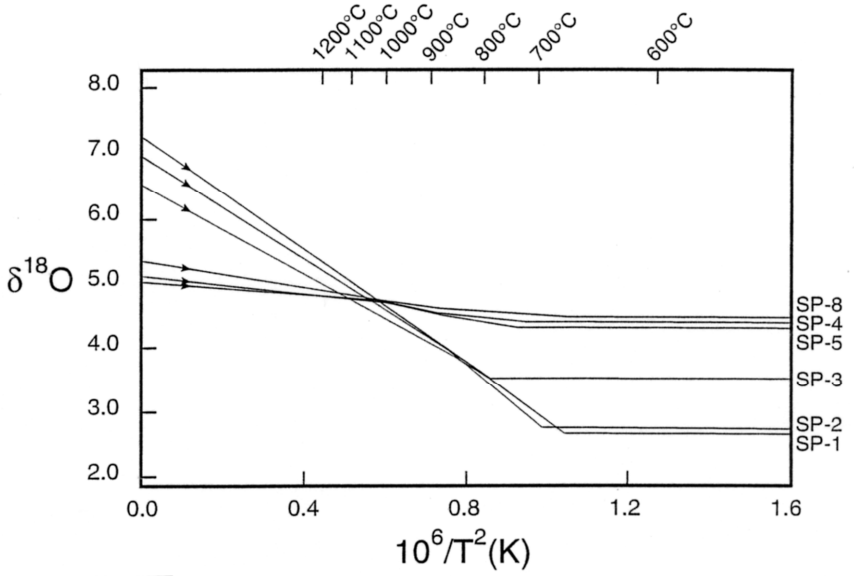

Figure 11. Isotope Exchange Trajectories (IET) for magnetite from six rocks from the Sybille Fe-Ti-oxide quarry, Laramie anorthosite complex. The average temperature of intersection, 1077±25°C, is higher than T_C for any mineral in these rocks, and it is interpreted as the solidus temperature of the magma (from Farquhar et al. 1993).

The IET approach can also be applied to multiple closely spaced hand samples if it is assumed that they were equilibrated with each other at the peak temperature (Farquhar et al. 1993, 1996). If each sample has different modal proportions, then the IET for any given mineral will be different in each lithology due to mass-balance effects. If the IET's for a single mineral are plotted together, they will intersect at the closure temperature for the multi-rock system, T_C(sys). T_C(sys) can be higher than T_C for any individual mineral. If more than two rocks are plotted, the redundant information serves as a check for

concordance (Fig. 11). Krylov and Mineev (1994) analyzed closely spaced samples of granulite and derived a temperature of 720°C, well above the mineral temperatures that were generally lower. Loucks (1996) presents an alternative graphical and arithmetic approach to multiple closely spaced hand samples such as banded gneisses and discusses applications for cation as well as isotope thermometry.

RAM thermometers

Diffusion modeling predicts that accurate thermometry can be obtained from Refractory Accessory Minerals (RAM, i.e. minerals resistant to the effects of temperature that are modally subordinate) if they occur in a rock that is modally dominated by a readily exchangeable mineral (i.e. the right side of Fig. 9). RAM thermometers can be applied without additional diffusion modeling, especially in nearly monomineralic rocks such as quartzite, marble, or anorthosite. The choice of accessory mineral is constrained to phases with T_C above the peak temperature of interest and may include minerals that are relatively common (garnet, pyroxene, olivine), have simple mineral chemistry (aluminosilicates, corundum, magnetite, graphite), and/or which can be dated (zircon, titanite, rutile, baddelyite, monazite). In the right matrix, many gems are appropriate including ruby/sapphire, tourmaline, diamond, or emerald. In lower temperature sedimentary or hydrothermal systems, minerals such as calcite, quartz and clays can serve as RAM thermometers if a fluid with known isotope ratio is the dominant isotope reservoir.

The basis of RAM thermometry is that the accessory mineral preserves the isotope ratio from crystallization because of slow diffusion, while the dominant mineral preserves its isotope ratio by mass-balance because there are no other sufficiently abundant, exchangeable phases. This assumes that the accessory mineral does not exchange by some faster process such as recrystallization. A number of tests can be applied for recrystallization such as imaging by optics, CL, BSE, IR, X-ray mapping, or chemical etching. Applications of these tests are discussed in later sections. Accuracy is improved if the refractory mineral is not abundant as this minimizes the exchangeable reservoir near its grain boundaries. This approach assumes that the rock has been a closed system with respect to the element of interest, and there is no growth zonation, cryptic alteration, or recrystallization of the RAM.

There are a large number of potential RAM thermometers and some guidelines and tests evaluate which are best in a certain situation. Mineral pairs with a large fractionation will generally have a larger temperature coefficient and the effects of analytical uncertainty are minimized. This consideration favors rocks where relatively high $\delta^{18}O$ minerals such as calcite, quartz, or feldspar are the exchangeable phase. Growth zonation of isotope ratio can be evaluated by microanalysis (graphite, Wada 1988; garnet, Kohn et al. 1993, 1994; Chamberlain and Conrad 1993); by comparison of large vs. small crystals (Valley and Graham 1991, Sharp 1991, Kitchen and Valley 1995, Edwards and Valley 1998); or by analysis of rocks with different mineral proportions (kyanite-quartz, Putlitz et al. 2001). Partial or complete recrystallization of the RAM after the event of interest can be evaluated by microanalysis (magnetite, Valley and Graham 1993, Eiler et al. 1995a,b, Sitzman et al. 2000; quartz, Graham et al. 1996, Valley and Graham 1996; calcite, Graham et al. 1998); or by geochronology (zircon, Valley et al. 1994, Peck et al. 2001; titanite, King et al. 2001).

One variant of RAM thermometry applies to rocks with more than one exchangeable mineral, but a single refractory mineral, such as sphene in a quartzo-feldspathic gneiss or granitoids, or garnet in granulite facies gneiss (Hoernes et al. 1995). An average fractionation factor is calculated for the exchangeable minerals based on mode and this

exchangeable reservoir is compared to the refractory mineral. This approach has the advantage of being applicable to many more common rocks than the strict RAM thermometer described above, but the use of whole rock data has the disadvantage that temperature sensitivity is reduced by averaging of high and low $\delta^{18}O$ minerals, and open system retrograde fluid effects are more commonly problematic due to analysis of all components of the rock.

Microscopic versus macroscopic models

The development of accurate techniques for microanalysis of stable isotope ratios permits studies of intra-crystalline zonation and applications of isotope exchange models at the microscopic scale. For isotopically complex samples, these results can differ significantly from macroscopic models that depend on averaged, bulk-mineral data. However, if minerals are homogeneous or have exchanged by a well-understood process, then the added effort of detailed microanalysis may not be necessary. One goal of future studies will be to determine which samples, processes, and geologic environments require microanalysis and which can reliably be interpreted with more rapid analysis at the macroscopic scale.

There are a number of processes that create fast pathways of exchange and effectively short-circuit volume diffusion into a crystal. Thus, the "real world" may be influenced by crystal defects and dislocations, mineral inclusions, exsolution lamellae, kink bands, microcracks, and other cryptic features (Fig. 12C). Diffusion is always active on a scale that can be modeled (Fig. 12B) and thus a world-view where all minerals are perfectly equilibrated and homogeneous (Fig. 12A) is generally a figment of imagination. In thermometry, these factors all potentially contribute to the compositions that are measured. Major advances have been made in determining when the macroscopic "model world" accurately predicts the microscopic "real world" situation. However, more work may be necessary to accurately deconvolute complex cases and tests should always be applied to evaluate thermometry.

TESTS OF THERMOMETRY

Concordance

The concordance test is commonly applied to evaluate equilibrium and the accuracy of stable isotope thermometry (Bottinga and Javoy 1975, Deines 1977). For three

Figure 12. Cartoons of minerals showing gradients of isotope ratio due to exchange in shades of gray. (A) the "imaginary world" where all minerals are homogeneous and equilibrated, and there are no gradients. (B) the idealized "model world" where exchange takes place radially inward from grain boundaries by diffusion. Actual gradients would be smooth. (C) the "real world" will show effects of diffusion and may also have fast pathways of exchange due to recrystallization, micro-cracks, dislocations, inclusions or deformation.

minerals in equilibrium, a plot of Δ_{i-j} vs. Δ_{j-k} will be a smooth curve. However, this is a necessary but not sufficient criterion. The calibrations of Δ_{i-j} and Δ_{j-k} vs. T should be independently known (Clayton 1981). Furthermore, a correlation can be observed even though individual samples may plot substantially off the equilibrium line because processes of resetting may be systematic (e.g. Giletti 1986, Eiler et al. 1992, 1993; Cole and Chakraborty, this volume).

In practice, concordance should be judged based on units of $\delta^{18}O$ (‰) rather than temperature (Deines 1977). For example, an uncertainty in Δ_{i-j} of ±0.2 ‰ would yield a large temperature uncertainty for high temperature minerals with small fractionations like sanidine and quartz, but ±0.2 ‰ would seem very accurate for a system that is quite sensitive to temperature variation such as Δ(quartz-magnetite).

δ-δ and δ-Δ diagrams

A number of papers have explored the use of δ_i vs. δ_j diagrams for determining the extent of isotope disequilibrium and open system fluid exchange (Gregory and Criss 1986, Gregory and Taylor 1986a,b; Criss et al. 1987, Gregory et al. 1989). Figure 13 plots $\delta^{18}O$(feldspar) vs. $\delta^{18}O$(pyroxene) for hydrothermally altered gabbros (Criss et al. 1987). Under equilibrium magmatic conditions, these minerals would have small high temperature fractionations falling along an array with slope = 1. The steeper slopes shown here result from open system hydrothermal alteration which has affected feldspar more extensively than pyroxene.

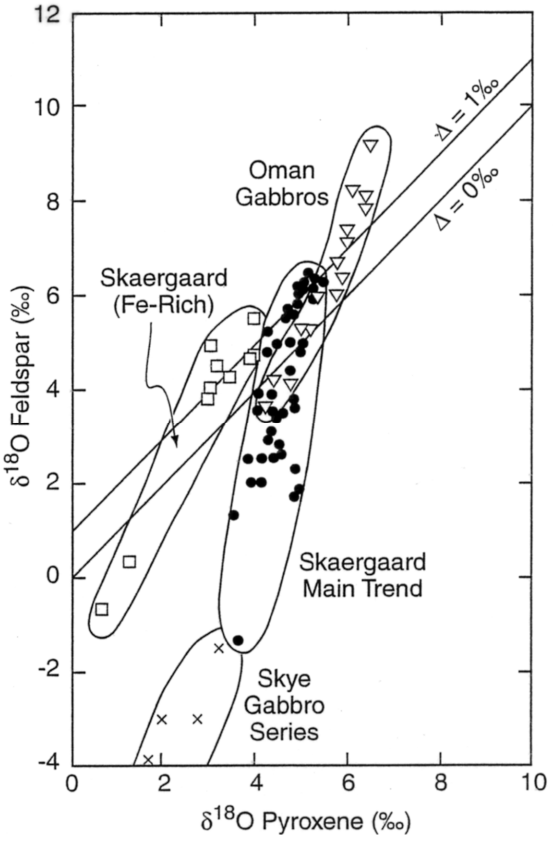

Figure 13. A plot of $\delta^{18}O$(fdsp) vs. $\delta^{18}O$(pyroxene) for various gabbros. If equilibrated at magmatic temperatures, these minerals would form a linear array with small fractionation and a slope of 1. The steeper slope and highly variable fractionations shown here indicate that the rocks have been altered by infiltration of hydrothermal fluids and that feldspar has exchanged more completely than pyroxene. (from Criss et al. 1987).

Several papers discuss the uses and pitfalls of δ_i vs. Δ_{i-j} diagrams (Shelton and Rye 1982, Ohmoto 1986, Gregory and Criss 1986, Gregory et al. 1989). Zheng (1992) compares δ-δ and δ-Δ diagrams for calcite- graphite thermometry.

Imaging

Imaging often reveals processes that reset stable isotope thermometers or that short-circuit pathways of exchange such that diffusion models do not apply. Optical examination may show evidence of: inclusions including exsolution lamellae, crack healing cements, late mineral growth on grain boundaries, deformation lamellae, or kink bands (Fig. 12C). If not visible optically, these textures and other more cryptic features such as dislocations, subtle chemical zoning, or sub-microscopic porosity may be detected by use of: X-ray diffraction, back-scattered electron imaging, secondary electron microscopy (Waldron et al. 1994), transmission

electron microscopy (Farver and Yund 1999, Sitzman et al. 2000), hot or cold cathode cathodoluminescence (Valley and Graham 1996, Graham et al. 1998), chemical etching (Eiler et al. 1995a, King et al. 1998), ion milling (Valley and Graham 1993, Sitzman et al. 2000), infra-red spectroscopy (Johnson et al. 2000), or elemental mapping by electron or ion microprobe (Walker 1990). In addition to identifying processes of alteration, X-ray imaging by electron microprobe can reveal cation zonation which affects isotope fractionation or correlates to isotope zonation (Kohn et al. 1993). The inherent assumptions of thermometry imply that samples be "well-behaved," i.e. relatively devoid of these features. When observed, such features can aid interpretation of stable isotope data to elucidate otherwise unrecognized events. The importance of carefully looking at one's samples cannot be over emphasized.

The outcrop test

The simplest and most direct test of thermometry is the outcrop test. This is a necessary but not sufficient criterion for accurate thermometry. If temperature estimates from a small area of constant T do not agree, the lack of self-consistency proves that there is a problem in interpretation. Conversely, if temperatures are self-consistent, especially for a suite of samples that spans a range of $\delta^{18}O$ values, this is commonly interpreted as strong support that a thermometer is working. However, precision does not prove accuracy, and other interpretations should still be evaluated.

Table 2. Outcrop tests for self-consistency in calcite-graphite (Cc-Gr) thermometry from Adirondack marbles (Kitchen and Valley 1995).

Locality	*Facies*	*$\Delta^{13}C$(Cc-Gr)*	*n*	*T(°C) ±1 std dev* [a]
Train Wreck	amphibolite	4.2± 0.2‰	5	652± 13
Fish Creek	amphibolite	4.0± 0.4‰	29	660± 29
Valentine Mine	amph/gran	3.8± 0.3‰	9	677± 21
Bloomingdale	granulite	3.2± 0.1‰	8	722± 9
Willsboro	granulite	3.1± 0.1‰	3	738± 11

[a] Temperature calculated from Dunn and Valley (1992).

Kitchen and Valley (1995) report $\Delta^{13}C$(calcite-graphite) temperatures for 144 amphibolite and granulite facies marbles from the Adirondacks, including outcrop tests at five localities (Table 2). Each outcrop was smaller than 100m in dimension. For a regional metamorphic terrane such as the Adirondacks, peak temperature is expected to be constant on this scale. Four of the Adirondack outcrops yielded reproducible temperatures within ±10-20°C, however, samples adjacent to the Fish Creek alaskite body (leucogranite) were more variable, ±29°C. This contact was investigated in depth because of controversy whether the metamorphosed alaskite was originally deposited as rhyolite or intruded as granite (McLelland et al. 1992). To explore the cause of the ±0.36 ‰ variability in $\Delta^{13}C$(Cc-Gr) at Fish Creek, calcite was microsampled from the 5-cm^3 domains that were analyzed for Cc-Gr thermometry and heterogeneity was found to range from 0.0 to 0.30 ‰. Subsequent examination of thin sections by cathodo-luminescence (CL) revealed that the heterogeneity in $\delta^{13}C$ is caused by variable amounts of late-stage calcite veining that is common in this area. Late calcite veining is commonly seen by CL in granulite facies orthogneisses (Morrison and Valley 1991) and marbles (Graham et al. 1998), and may degrade the precision and accuracy of thermometry elsewhere.

Microanalysis

Analysis at the appropriate scale for thermometry often requires very small samples, either as mineral separates, chips, or *in situ*. Table 1 reviews techniques for stable isotope microanalysis and Figure 1 shows the analytical trade-offs for different systems of microanalysis as they are generally applied in 2001: ion microprobe analysis; IR-wavelength laser fluorination of chips or powder; UV-wavelength laser analysis *in situ*; and continuous flow mass-spectrometry (CFMS) which can be coupled to pyrolysis or laser systems.

Laser heating, fluorination, or vaporization is increasingly used for isotope analysis. A variety of wavelengths have been employed from mid-IR (λ = 10.6 μm) to UV (0.266-0.157 μm, Kelley and Fallick 1990, Sharp 1990, Crowe et al. 1990, Farquhar and Rumble 1998, Eiler unpbd., see Rumble and Sharp 1998, Shanks et al. 1998). *In situ* analysis of oxygen or sulfur by IR laser yields a rind of partial reaction and fractionation encircling the laser pit. These edge effects can be corrected for sulfur isotopes (Crowe et al. 1990), but lead to degraded precision for oxygen (Elsenheimer and Valley, 1992). Analysis of mineral separates is quantitative and removes fractionation due to edge effects. The CO_2 laser (10.6 μm) yields the best accuracy and precision of any technique for $\delta^{18}O$ in silicate and oxide minerals when applied to 1-2 mg of mineral separate. Significant other advantages include ability to analyze refractory minerals, speed, and reliability of analysis, and better standardization (Sharp 1992, Valley et al. 1995).

Mineral separates for laser analysis can be prepared in a number of ways so as to micro-sample specific features in a single crystal or to concentrate a specific region from many similar crystals. Thin diamond saw blades can easily cut a checkerboard of chips from specially prepared thick microscope sections permitting correlation of $\delta^{18}O$ to optical or electron microprobe imaged features (Elsenheimer and Valley 1993). Over 200 analyses per square centimeter are possible by this approach (Kohn et al. 1993). Carbide or diamond tipped drills can be precisely controlled by computer. In soft minerals, elongate features as thin as 10-20 μm can be sampled if length is sufficient for sample needs (Patterson et al. 1993). Soft minerals can also be shaved at the 10-20 μm-scale by microtome (Wada 1988). Minerals with good cleavage like mica or graphite can be delaminated at scales less than 100 μm with a razor blade (Wada 1988, Kitchen and Valley 1995). Air abrasion permits analysis of cores or thin overgrowths on equant minerals such as zircon (Bindeman and Valley 2000) or pyroxene (Edwards and Valley 1998). For minerals that dissolve congruently without residue, partial etching in acid can remove unwanted features without compromising accuracy. HF etching removes overgrowths and cements on quartz (Forrester and Taylor 1977, Graham et al. 1998) and zones of radiation damage in zircon (King et al. 1998).

In situ analysis by UV laser is more precise than *in situ* analysis by IR because there is less heating (see Rumble and Sharp 1998, Farquhar and Rumble 1998, Young et al. 1998, Fiebig et al. 1999, Jones et al. 1999). The spot diameter of a UV laser and the sample size of a continuous flow mass-spectrometer can rival that presently used for oxygen isotope analysis by ion microprobe, however, the spatial resolution by laser is limited by the quantity of oxygen necessary for accurate purification during conversion of mineral to gas. At present, the analytical precision and the spot size attainable by *in situ* lasers are intermediate between the capabilities of the ion microprobe (best spatial resolution) and the CO_2 laser (best precision and accuracy, Fig. 1). For some projects this offers the best analytical compromise.

The best spatial resolution for stable isotope analysis is obtained by ion microprobe, but at a trade-off against precision (see Valley et al. 1998a, McKibben and Riciputi 1998,

McKeegan and Leshin, this volume). Typically, spot size is 10-30 μm in diameter and 1-5 μm deep. Over short distances normal to a flat surface, sub-micron spatial resolution is possible by depth profiling (Valley and Graham 1991). The recent development of multiple collectors for ion microprobes has lead to a major reduction in analysis time and promises enhanced accuracy and precision.

Ion microprobe analysis has an additional advantage over *in situ* analysis by UV laser. Even in the absence of any edge effect, *in situ* laser analysis of silicates requires that the entire sample be immersed in fluorinated gas and that only the area of laser illumination reacts to liberate oxygen. This situation may be met for a few rocks, but most rocks contain minor amounts of highly reactive material along grain boundaries and many rocks contain one or more minerals that are reactive at such low temperatures that pre-reaction of unlased material occurs leading to unavoidable sample contamination. Elsenheimer and Valley (1992) coated thin wafers with gold prior to laser analysis, but high blanks were still a problem for many rocks. Thus, background blanks should be carefully evaluated and reported for *in situ* laser data. In contrast, the zone of ion microprobe sputtering is well defined, and with proper precautions, no significant signal is derived from outside the pit.

Correlations to mode or crystal size

For minerals that have not equilibrated, isotope ratio may correlate to the size of an individual crystal. Growth zonation is to be expected in metamorphic minerals such as garnet due to temperature change during growth (Kohn et al. 1993) or in magmatic phenocrysts such as zircon due to evolving magma chemistry (Bindeman and Valley 2000). Retrograde exchange by diffusion causes concentric zonation affecting smaller crystals more than large crystals due to the difference in surface area/ volume. Thus, $\delta^{18}O$ has been shown to correlate with crystal size for metamorphic magnetites (Valley and Graham 1991, Sharp 1991), diopside (Edwards and Valley 1998, but see Sharp and Jenkin 1994), graphite (Kitchen and Valley 1995), and detrital zircons in granulite facies quartzite (Valley et al. 1994, Peck et al. 2001). Thus a correlation of isotope ratio to crystal size indicates a departure from the requirements of accurate thermometry and should be avoided for that purpose.

The Fast Grain Boundary diffusion model predicts that retrograde exchange will create correlations of isotope ratio to the modal proportions of a rock (Figs. 9 and 10; Eiler et al. 1993). These predictions have been verified for a range of amphibolite to granulite facies rocks (Hoffbauer et al. 1994, Eiler et al. 1995a,b; Farquhar et al. 1996, Edwards and Valley 1998, Ghent and Valley 1998, Putlitz et al. 2001). Mode effects also indicate pertur-bations that should be avoided for thermometry, but which may be useful for other studies. Knowledge of such correlations can distinguish polymetamorphic overprints, or estimate the rate of diffusive exchange or cooling. In turn, understanding retrograde kinetics may permit retrograde effects to be avoided and more accurate thermometry to result.

OXYGEN ISOTOPE THERMOMETRY

RAM thermometers

Several oxygen isotope Refractory Accessory Mineral (RAM) thermometers have been applied, including aluminosilicate, magnetite, garnet, or rutile in quartzite; and magnetite, titanite or diopside in marble. Graphite in marble forms a commonly applied RAM carbon isotope thermometer. It is important to keep in mind that all thermometers have an optimum temperature range for applicability. The peak temperature should be below the closure temperature of the RAM. However, for some minerals, at temperatures

too far below T_C, the possibility of growth zoning becomes greater.

Refractory minerals are defined based on the relative diffusion rates of the RAM vs. its matrix. Thus Δ(Plag-Mt) or Δ(Plag-Rt) may be excellent RAM thermometers in amphibolite or eclogite facies anorthosites or metabasalts, but fail in the granulite facies. Likewise, Δ(Qt-Mt) and Δ(Cc-Mt) should be used with caution because of the smaller, possibly reversed, contrast in diffusivity. Diffusion data and values of T_C are given in Table 3 as a quick guide for choosing an appropriate thermometer. Cole and Chakraborty (this volume) provide a more detailed presentation of stable isotope diffusion data and exchange kinetics. However, such theoretical predictions do not, at present, consider the full complexity of the real world. There is no substitute for careful measurements.

Table 3. Diffusion characteristics (D_o, E) and closure temperature (T_o; Eqn. 9) for minerals useful in stable isotope thermometry. Cooling rate is varied from 1°C/Ma to 106°C/Ma for a mineral radius of 0.1 mm.*

Mineral	Orientation	P(H2O)	Reference	D_o cm^2/s	E KJ/mol	A	T_c °C * 1C/Ma	T_c °C * 10^2C/Ma	T_c °C * 10^4C/Ma	T_c °C * 10^6C/Ma
OXYGEN										
anorthite	~isotropic	1 Kb	Giletti et al. 1978	1.39E-07	109.6	55	150.7	218.7	311.7	445
anorthite		dry	Elphick et al.	9.00E-06	234.3	55	515	624	766.5	961
anorthite	//(010)	dry	Ryerson+McKeegan 1994	8.40E-09	162	55	402.5	520.1	684.7	931
apatite	//C	1 Kb	Farver and Giletti 1989	9.00E-05	205	55	378.9	463.9	573.4	719
biotite	//C	1 Kb	Fortier and Giletti 1991	9.10E-06	142.2	8.7	236.6	312.1	412.8	553
calcite	~isotropic	1 Kb	Farver 1994	7.00E-05	173	55	283	356.3	451.1	578
calcite	~isotropic	dry	Labotka et al. 2000	7.50E-03	242	55	416.9	496.9	597.4	727
corundum	//C		Cawley 1984	1.51E+01	527	55	989	1111	1258	1439
diopside	//C	dry	Ryerson+McKeegan 1994	4.30E+00	457	55	851.4	963	1099	1267
diopside	//C	1 Kb	Farver 1989	1.50E-06	226	55	525.6	642.1	796.7	1011
garnet	isotropic	wet	Coghlan 1990	6.00E-05	301	55	684.7	809.5	970.5	1185
hornblende	//C	1 Kb	Farver and Giletti 1985	1.00E-07	171.5	8.7	426.4	545.4	710.6	954
kyanite		1 Kb	est. *	8.60E-06	363.1	8.7	996.9	1180	1422	1757
magnetite	isotropic	1 Kb	Giletti and Hess 1988	3.50E-06	188.3	55	380.4	473.7	597.3	767
Mg-spinel	isotropic		Ryerson+McKeegan 1994	2.20E-03	404	55	897.6	1036	1210	1435
muscovite	//C	1 Kb	Fortier and Giletti 1991	7.70E-05	163.2	8.7	276.7	352.9	452.6	588
phlogopite	//C	1 Kb	Fortier and Giletti 1991	1.40E-04	175.7	8.7	308.5	387.4	490.5	630
quartz	//C	1 Kb	Dennis 1984a	2.00E-07	138.1	8.7	281.8	374.6	503	691
quartz		dry	Dennis 1984b	3.00E-07	221.8	8.7	594.1	735.1	928.1	1207
quartz	//C	dry	Sharp et al. 1991	2.10E-08	159	8.7	410.9	534.2	708.7	973
richterite	//C	1 Kb	Farver and Giletti 1985	3.00E-04	238.5	8.7	494.9	596.2	727.4	903
rutile	//C	1 Kb	Moore et al. 1998	5.90E-01	330	8.7	611	707	825.8	976
sillimanite		1 Kb	est. *	6.20E-07	254.5	8.7	696.4	849.5	1058	1355
sphene	isotropic	1 Kb	Morishita et al. 1996	1.00E-04	254	55	528.3	631.8	765	942
tremolite	//C	1 Kb	Farver and Giletti 1985	2.00E-08	163.2	8.7	429.4	556.1	735.6	1008
zircon	~isotropic	70-700 b	Watson+ Cherniak 1997	5.50E-08	210.2	55	546.4	679.2	861.1	1124
zircon	~isotropic	dry	Watson+ Cherniak 1997	1.33E+00	448.3	55	856.5	971.4	1112	1287
zircon		empirical	Peck et al. 2001				>700	>700	>700	>700
CARBON										
calcite	~isotropic	**0.02-24 b**	Kronenberg et al. 1984	7.00E+02	364	55	544.3	618.1	706.2	813
calcite	~isotropic	dry	Labotka et al. 2000	7.77E-09	166	55	420.3	541.3	710.8	964
graphite	~isotropic		Thrower+ Mayer 1978	9.10E-01	651	55	1367	1534	1738	1993

***Footnotes:** Note that cooling rate scales inversely to radius squared in Eqn. (9). Thus, Tc for 10^6C/Ma and 0.1mm is equivalent to Tc for 10^4C/Ma and 1mm, 10^2C/Ma and 1cm, etc.
See Cole and Chakraborty (2001) for a discussion of alternate calibrations of D_o and E.
Do and A estimated by the technique of Fortier and Giletti 1989 (Ghent and Valley 1998).

Aluminosilicate-quartz

Assemblages of quartz plus kyanite, sillimanite or andalusite have yielded exceptionally precise and apparently accurate temperatures when applied as a RAM thermometer. Diffusion of oxygen in aluminosilicates is very slow, yielding $T_C > 800$°C for moderate to coarse grain sizes, while diffusion is comparatively fast in quartz (Table

3). The effects of solid solution are generally nil and the temperature coefficient relative to quartz is moderate (Zheng 1993b, Sharp 1995, Tennie et al. 1998).

Putlitz et al. (2001) analyzed coarse kyanite from deformed quartz veins in pelites from the kyanite (+sillimanite) zone on the island of Naxos, Greece (Table 4). Six samples from an outcrop test within 100m at Stavros yielded highly precise fractionations (±0.06 ‰) and temperatures in excellent agreement with published estimates for coexisting kyanite + sillimanite. Temperatures above T_C(Qt) are preserved because there is not another low T_c mineral in the veins. The host pelitic rocks at Stavros also contain quartz and kyanite; however, Δ(Qt-Ky) is larger in pelites (3.03 vs. 2.62 ‰) due to diffusive exchange between quartz, feldspars, and micas yielding reset temperatures that are 65°C lower. Fibrolitic sillimanite was also analyzed from three samples at Stavros, yielding about the same average temperature, but more variable results (634-726°C), possibly reflecting exchange due to the fine grain size. Samples of Qt-Ky from other localities accurately reproduce the petrologic temperatures. These accurate and precise results demonstrate the potential of RAM thermometry.

Table 4. Aluminosilicate- quartz thermometry in quartzites, pelites, and quartz veins.

		Average		*Qt-AS*	*Independent*	
Ref.	*Location*	*Δ(Qt-AS)*	*n*	*Ave T**	*T estimate*	
1.	**Naxos, Greece, deformed quartz veins, coarse kyanite**					
	Stavros	2.62±0.06	6	659±11	660	
	Komiaki	2.48	1	685	670	
	Sifones	2.64	1	656	630	
	Moni	2.65	1	649	630	
	Appollon	2.76	1	635	630	
	Appollon Village	2.77	1	634	620	
2.	**Mica Creek, BC, pelites and quartz nodules**					
	Qt-Ky, nodule	2.55	2	665±10	645	Ky-Si zone
	Qt-Ky, pelite	3.0±0.24	4	596±35	637±28	St-Ky zone
	Qt-Ky, pelite	2.9±0.25	3	605±38	605±26	Ky-Si zone
	Qt-Si, pelite	2.7±0.25	3	648±43	702±23	Si zone

References: **1**. Putlitz et al. (2001); **2**. Ghent and Valley (1998).
* T calculated from Sharp (1995).

In an experimental study, Tennie et al. (1998) challenge the interpretations of Sharp (1995) and Ghent and Valley (1998) for aluminosilicate-quartz thermometry. They propose that the refractory nature of kyanite prevents metamorphic equilibration and makes kyanite generally unfit for thermometry. They estimated $A_{Qt\text{-}Ky}$ = 3.00 (Eqn. 4) based on 11 of 17 piston cylinder experiments for calcite-kyanite exchange, and analysis using externally heated nickel reaction vessels. This calibration yields higher temperatures than the A value empirically estimated by Sharp (A = 2.25, 1995). In many instances, temperatures based on A = 3.00 are in significant disagreement with independent estimates. For instance, at Stavros (Naxos, Table 4), the average temperature is raised from 659 to 797°C. At 797°C, there should be widespread melting in these water-rich metasediments, but no evidence of *in situ* melting is observed on Naxos except at much higher grade. Tennie et al. ascribe such discrepancies to slow diffusion in kyanite (see Table 3) which could prevent exchange and cause kyanite to preserve $\delta^{18}O$ from the lower temperatures of first crystallization rather than the peak of metamorphism. However, this explanation would yield Qt-Ky temperatures in quartzite that are too low rather than too high as is observed, and it does not explain the excellent agreement of

results from six different hand samples in the outcrop test at Stavros (Table 4).

Discrepancies between empirical and experimental calibrations exist for several systems, including quartz-alumino-silicate. In this case, one should ask if an empirically derived thermometer falsely seems to record accurate temperature because the rocks used for calibration were retrogressed by an equal amount as those being studied, or if all rocks really preserve equilibrium compositions. This distinction is important because a non-equilibrated system cannot be relied upon and unequilibrated apparent temperatures may actually be controlled by other variables such as fluid composition, time, or deformation. Conversely, if careful thermometry yields self-consistent results in agreement with other systems, as concluded by Sharp (1995), Ghent and Valley (1998), Vannay et al. (1999), and Putlitz et al. (2001), then it may be that the experiments are in error.

Values of $\Delta(\text{Qt-Al}_2\text{SiO}_5)$ can yield more than temperature information. Larson and Sharp (2000) analyzed coexisting quartz + sillimanite + kyanite + andalusite to show that "triple-point" assemblages from New Mexico did not form in equilibrium. Texturally equilibrated quartz + andalusite + sillimanite from the Front Range, Colo, yield estimates of pressure as well as temperature (Cavosie et al. 2000). Quartz + kyanite and quartz + sillimanite pairs from British Columbia yield precise temperatures from quartz nodules, but lower reset temperatures from assemblages in poly-mineralic pelites (Table 4). Fast Grain Boundary diffusion calculations based on the difference between RAM and pelite temperatures suggest that water activity was low during slow retrograde cooling (Ghent and Valley 1998).

Other applications of quartz-aluminosilicate fractionations include migmatitic, amphibolite or granulite facies gneisses (van Haren et al. 1996, Kohn et al. 1997, Vannay et al. 1999, Moecher and Sharp 1999), and eclogites (Sharp et al. 1992, 1993; Rumble and Yui 1998, Zheng et al. 1998, 1999). Moecher and Sharp (1999) compared the results of aluminosilicate-quartz and aluminosilicate-garnet thermometry in pelites and report variable retrograde resetting as predicted by diffusion modeling.

Magnetite-quartz

The magnetite-quartz pair is the most commonly applied oxygen isotope thermometer. It is very promising as a RAM thermometer below T_C(Mt) or when used in low to moderate grade metamorphic, rapidly cooled, or very dry rocks. It is frequently discussed in reviews of isotope thermometry (O'Neil and Clayton 1964, Chiba et al. 1989, Gregory et al. 1989, Zheng and Simon 1991). The fractionation is large yielding good temperature sensitivity and the effects of solid solution and crystal chemistry are relatively small (Ti, Fe^{3+} in magnetite, Bottinga and Javoy 1975, Zheng and Simon 1991; SiO_2 polymorphs, Kawabe 1978, Zheng 1993b; spinel structure, Zheng 1995).

Rumble (1978) measured Mt-Qt fractionations from eight amphibolite facies quartzites on the summit of Black Mountain, New Hampshire. These closely-spaced samples were subjected to the same P-T-time conditions. All but one sample contains at least 80% quartz and smaller amounts of magnetite. Coexisting minerals indicate a peak metamorphic temperature of 530°C: kyanite + staurolite + chloritoid + chlorite + muscovite + quartz + magnetite ± ilmenite ± garnet. The fractionations are self-consistent (9.46±0.26‰) yielding nearly parallel tie lines (Fig. 14). The oxygen isotope temperatures range from 530-561°C (542±11, Table 5). This study is an outcrop test and demonstrates the accuracy and precision obtainable from Mt-Qt when applied to appropriate rocks for a RAM thermometer.

The magnetite/hematite-quartz thermometer has been extensively applied to banded

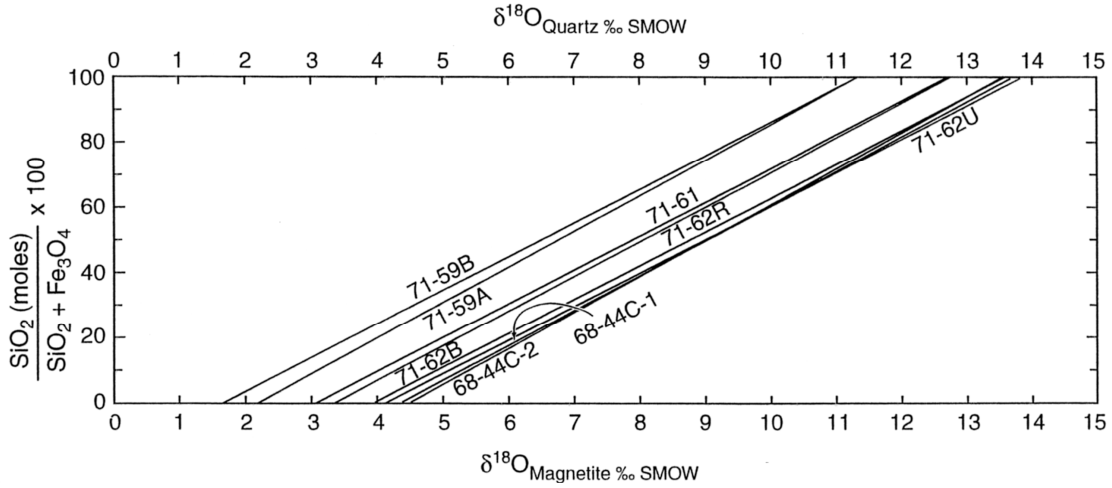

Figure 14. Plot of $\delta^{18}O$(magnetite) vs. $\delta^{18}O$(quartz) for amphibolite facies quartzites from Black Mtn., New Hampshire. The nearly parallel tie-lines indicate that fractionations are self-consistent for these eight samples from one outcrop. The average oxygen isotope temperature of 542°C is in excellent agreement with that from petrology (530°C). (from Rumble (1978).

Table 5. Comparison of $\Delta^{18}O$(Qt-Mt) temperature estimates from quartzite, granitic gneiss, and banded iron formation. Amphibolite facies Black Mtn. quartzite yields accurate and precise RAM temperatures. Granulite facies temperatures are often low relative to petrologic estimates.

Reference, Location	*Average Δ(Qt-Mt)*	*n*	*Ave T*[a] *°C*	*Comments*
1. Shuksan, N. Cascades	13.8±1.50	6	402±37	BSF, lawsonite, pumpellyite
2. Black Mtn., N.H., Qtzt,	9.46±0.26	8	542±11	AF, 530°C, 500 × 100 m, RAM
3. Isua, SW Greenland	11.62±0.42	12	463±13	AF, BIF, 1 × 2 km
4. Minas Gerais, Brazil	10.79±0.39	16	491±14	GSF, BIF, s_1 only[b]
	8.14±0.77	38	606±40	AF, BIF, s_1 only[b]
	6.32±0.41	9	724±33	GF, BIF, s_1 only[b]
	8.89±2.47	16	568±88	GF, BIF, $s_1+s_2+s_3$[c]
5. Ruby Range, Mont., Kelly	8.42±0.19	3	591±10	GF, 745±50°C, BIF, 1 km^2
Carter Creek	9.67±0.43	3	533±18	GF, 675±45°C, BIF, 9 km^2
6. Adirondack Mts, unsheared	6.93±0.58	11	680±38	GF, 675-700°C, GG
sheared	8.8±1.22	11	603±71	GF, 675-700°C, GG
7. Wind River Range, Wyoming	9.24±0.93	16	552±44	GF, 750±50°C, BIF

References: 1. Brown and O'Neil (1982), 2. Rumble (1978); 3. Perry et al. (1978); 4. Muller et al. (1986b); 5. Dahl (1979); 6. Cartwright et al. (1993); 7. Sharp et al. (1988); Sharp and Essene (1991).

Footnotes: [a] calculated using the calibrations of Chiba et al. (1989); [b] data only for samples of magnetite/hematite showing primary schistosity s_1; [c] data for samples of magnetite/hematite with variable schistosity s_1, s_2, or s_3

Abbreviations: AF = amphibolite facies; BIF = banded iron formation; BSF = blueschist facies; GF = granulite facies; GG = granitic gneiss or charnockite; GSF = greenschist facies; RAM = refractory accessory mineral thermometer; Qtzt = quartzite.

iron formations in order to determine conditions of deposition, diagenesis and metamorphism: Animikie Basin, U.S. (Clayton and Epstein 1958, James and Clayton 1962); Duluth gabbro contact aureole, U.S. (James and Clayton 1962, Perry and Bonnichsen 1966); Hamersley Basin, Western Australia (Becker and Clayton 1976); Isua, SW Greenland (Perry et al. 1978); Krigoy Rog, Ukraine (Perry and Ahmad 1981); Mesabi

Range, U.S. (James and Clayton 1962, Perry et al. 1973); Minas Gerais, Brazil (Hoefs et al. 1982, Muller et al. 1986a,b); Ruby Range, Montana (Dahl (1979); Urucum area, Brazil (Hoefs et al. 1987); and the Wind River Range, Wyoming (Sharp et al. 1988, Sharp and Essene 1991). These data include samples from different metamorphic grades: unmetamorphosed to sub-greenschist (Animikie, Hamersley, Mesabi, Urucum); greenschist facies (Krivoy Rog, Minas Gerais); amphibolite facies (Isua, Minas Gerais); granulite facies (Minas Gerais, Ruby Range, Wind River); and contact metamorphism (Duluth gabbro aureole). Reexamination of these samples, using more recent criteria for thermometry, can be expected to yield improved accuracy. The temperatures found by these studies should be recalculated with newer experimental data (Chiba et al. 1989, Clayton et al. 1989). Furthermore, it is possible that isotope heterogeneity exists at the scale of the large samples analyzed, and that equilibrated domains can be identified and analyzed with microanalysis.

Magnetite-quartz thermometry has also been applied in igneous rocks (Hildreth et al. 1984, Bindeman and Valley 2001) and high grade gneisses (Fourcade and Javoy 1973, Shieh and Schwarcz 1974, Shieh et al. 1976, Li et al. 1991, Cartwright et al. 1993, Hoffbauer et al. 1994, Farquhar et al. 1996), blueschists (Brown and O'Neil 1982), and greenschist or amphibolite facies pelites (Schwarcz et al. 1970, Hoernes and Friedrichsen 1974, Kerrich et al. 1977, Goldman and Albee 1977).

There are several cautionary notes for thermometry involving Fe-Ti oxides and quartz. Minerals may differentially exchange with circulating fluids as clearly demonstrated by Gregory et al. (1989) with $\delta^{18}O$(Qt) vs. $\delta^{18}O$(Mt) plots. For Hamersley and Mesabi, it is proposed that sedimentary Fe-oxides exchanged with fluids during recrystallization to magnetite, while quartz remained unaffected. The calibration of $1000\ln\alpha^{18}O$(Qt-Mt) vs. T is uncertain at low temperatures. Values of Δ(Mt-hematite) and Δ(ilmenite-Mt) are small, but not insignificant (Bottinga and Javoy 1975, Zheng 1991, Zheng and Simon 1991). In Ti- or Fe^{+3}-rich oxides, exsolution effects are minimized for lower grade rocks, but may be significant in granulites (Bohlen and Essene 1977, Farquhar and Chacko 1994). Fine grain size has sometimes precluded complete mineral separation and various projection schemes have been applied to banded iron formation (see, Yapp 1990). The moderate diffusion rates of oxygen in both quartz and magnetite, and measured fractionations indicate that temperatures will be reset above T_C, for granulite and upper amphibolite facies rocks (Chiba et al. 1989, Valley and Graham 1991, Sharp 1991, Sharp and Essene 1991, Eiler et al. 1993, 1995a,b). In addition to diffusive processes that operate in all samples, both magnetite and quartz can exchange $\delta^{18}O$ by recrystallization or crack-healing (Valley and Graham 1993, 1996; Eiler et al. 1995a, Sitzman et al. 2000). Likewise, different generations of quartz are recognized from textures in Archean Onvervacht cherts and small differences in $\delta^{18}O$ have been measured (Knauth and Lowe 1978).

In spite of the many potential pitfalls, Mt-Qt is an accurate and reliable thermometer when carefully applied to appropriate rocks in an appropriate temperature regime. Samples should be selected with regard to diffusive exchange, discussed above. Temperature estimates are consistent with petrology for blueschist, greenschist and lower amphibolite facies samples in Table 5. In spite of the moderate T_C for both quartz and magnetite (Table 3), some granulite facies gneisses preserve peak metamorphic temperatures (Muller et al. 1986b, Cartwright et al. 1993) and others yield temperatures that are reset, but higher than T_C (Sharp et al. 1988). However, most granulite and upper amphibolite facies samples yield temperatures that are too low in comparison to petrologic thermometers, though reset results can be precise (Table 5). The variable retention of peak temperature is predicted if water fugacity is low (promoting slow

diffusion) in some rocks *during cooling*, but high in others (Sharp et al. 1988, Cartwright et al. 1993, Edwards and Valley 1998). Improved results have been obtained through careful attention to rock and mineral fabric in regionally metamorphosed terranes (Muller et al. 1986a, Sharp et al. 1988, Cartwright et al. 1993). Crystal dislocations in magnetite that can facilitate retrograde oxygen exchange are easily seen in polished thin sections that have been etched in HCl (Valley and Graham 1993, Eiler et al. 1995b, Sitzman et al. 2000). Healed microfractures in quartz, if present, are often imaged by cathodo-luminescence using a SEM or electron microprobe, though sensitivity varies greatly with instrument and operating conditions (Valley and Graham 1996).

Rutile-quartz

The Ru-Qt thermometer has the same theoretical advantages as Mt-Qt. The temperature coefficient of fractionation is large and solid-solution is minor. The greatest limitation of this system may be the rate of oxygen diffusion (Table 3).

Quartz-rutile pairs have been measured most commonly from eclogites (Vogel and Garlick 1970, Desmons and O'Neil 1978, Matthews et al. 1979, Agrinier et al. 1985, Agrinier 1991, Sharp 1995, Rumble and Yui 1998, Zheng et al. 1998, 1999). A few analyses are reported for blueschists and pelites (Matthews and Schliestedt 1984, Sharp 1995), and nelsonite (Addy and Garlick 1974). Vogel and Garlick (1970) report very high precision: Δ(Qt-Ru)= 6.46±0.05‰ for 5 unrelated type B eclogites (609±4°C, Matthews 1994) and 7.30‰ for one type C (556°C). However, other studies are less sucessful. Sharp (1995) reports analyses from five granulite facies samples from terranes where the reported temperatures average 755°C and Δ(Qt-Ru) yields average temperatures of 567±150°C. The only granulite that yields above 700°C is a rapidly quenched xenolith from La Joya Honda maar. Plots of Δ(Qt-Ru) vs. Δ(Qt-garnet) and Δ(Qt-Ru) vs. Δ(Qt-kyanite) for the data referenced above show considerably larger scatter than Δ(Qt-garnet) vs. Δ(Qt-kyanite) for the same rocks, suggesting that in spite of the smaller temperature sensitivity, these other pairs may be more reliable. The effect of diffusion cannot be predicted for most of these samples without information on modes and grain size that is not published. Furthermore, rutile has the unusual property that hydrous experiments yield slower diffusion coefficients than dry experiments in the same lab (Moore et al. 1998). Since quartz is a minor phase in many of these mafic rocks, it is likely that variable resetting to lower temperatures has occurred by exchange with micas or chlorite. In a few samples with high Qt-Ru temperatures, it is possible that retrograde fluids were present.

Rutile is common in certain quartz veins, quartzites, and some massif-type anorthosites. These assemblages should be sought as a test of the RAM thermometers. Within the temperature range dictated by diffusion in rutile (Table 3) it is predicted to be highly accurate and precise.

CARBON ISOTOPE THERMOMETRY

Calcite-graphite

Cc-Gr is the most commonly applied RAM thermometer (Table 6). The percentage of graphite is generally less than 1% in marble, other carbon-bearing phases such as scapolite or dolomite are usually minor in abundance, and the diffusion rate of carbon is very slow. Furthermore, Δ(Cc-Scap) and Δ(Cc-Dol) are small at high temperatures, minimizing the effect of neglecting small amounts of these minerals. With routine care, this is an easily applied and accurate thermometer for high-grade marbles.

A number of empirical, experimental or theoretical calibrations of Δ^{13}C(Cc-Gr) vs. T

Table 6. Comparison of $\Delta^{13}C$(Cc–Gr) temperature estimates (°C) from granulite and amphibolite facies terranes.

Ref. *Location*	*Average Δ(Cc–Gr)*	*n*	*Cc-Gr K+V*	*Ave T's*[b] *D+V*	*Independent estimate T °C*[c]
1. Anabar Shield, Russia	3.83	4	691	677	<850-950 gf
2. Bohemian Massif	4.81	9	590	613	700-780, 530-620
3. Central Adirondack Mtns.	3.44[a]	38	744	707	675-775 gf
near anorthosite	3.02	17	813	743	polymetamorphic[d]
4. Central Adirondack Mtns	3.49	10	737	703	675-775 gf
5. NW Adirondacks	4.08	89	661	659	<675 af
6. Cucamonga terrane, California	3.54	10	746	705	710-820 gf
7. Franklin marble, amph. facies	3.60	3	722	695	af
gran. facies	3.09	3	801	737	gf
8. Gour Oumelalen, Algeria	3.45	10	743	706	≥710 gf
9. Hida Belt, Japan	3.46	5	742	706	polymetamorphic[d]
10. Ivrea Zone, Italy	4.9-2.3	14	580-970	600-800	
11. Kamioka area, Japan	3.54	40	729	699	
12. Kerala Belt, S. India	3.33	10	760	716	650-750 gf
13. Kurobegawa area, Japan	5.77	9	513	560	St+Ky af
14. Lutzow Holm Bay, E Antarctica	2.85	2	845	759	700-800 gf
15. Madurai, southern India	2.67	18	881	776	Sap+Qt gf
16. Panamint Mtns, marbles	6.40	17	473	530	400-650 af
schists	8.78	18	364	441	400-650 af
17. Sanbagawa terrain, Japan	8.37	15	379	455	500 Gt-zone af
18. Skallen marble, E. Antarctica	2.85	5	844	758	760-830 gf
19. Southern Grenville Province, ON	6.88	31	447	510	500-650 af
20. Sri Lanka, SW Group marbles	4.49	14	618	632	600-750 gf
21. Sri Lanka, granulite facies	3.79	19	696	680	gf
altered calcite	2.93	6	829	751	disequilibrium
22. Tudor Gabbro aureole, <1km	4.31	17	636	644	polymetamorphic
>1km	7.32	8	424	492	490 lower af
23. Madurai, Tamil Nadu	4.06	3	662	660	gf

References: 1. Galimov et al. (1990); 2. Schrauder et al. (1993); 3. Valley and O'Neil (1981), Kitchen and Valley (1995); 4. Weis et al. (1981); 5. Kitchen and Valley (1995), Gerdes and Valley (1994); 6. Morrison and Barth (1993) ; 7. Crawford and Valley (1990); 8. Pineau et al. (1976); 9. Arita and Wada (1990); 10. Baker (1988); 11. Wada (1977); 12. Satish-Kumar et al. (1997); 13. Wada (1977); 14. Satish-Kumar et al. (1998); 15. Satish-Kumar (2000); 16. Bergfeld et al. (1996); 17. Wada et al. (1984); 18. Satish-Kumar and Wada (2000); 19. Rathmell et al. (1999); 20. Elsenheimer (1988); 21. Hoffbauer and Spiering (1994); 22. Dunn and Valley (1992); 23. Pandey et al. (2000).

Footnotes: [a] does not include zoned, polymetamorphic graphites; [b] calculated using the calibrations of Kitchen and Valley (1995) and Dunn and Valley (1992); [c] some terranes contain gradients in metamorphic temperature and these differences are averaged; [d] graphites from plutonic contacts are zoned in $\delta^{13}C$.

Abbreviations: af = amphibolite facies, gf = granulite facies, Gt = garnet, Ky = kyanite, Qt = quartz, Sap = sapphirine, S t= staurolite

have been proposed (Fig. 15). Kitchen and Valley (1995) compared 38 measured fractionations with petrologic thermometry for granulite facies metamorphism of the central Adirondack Highlands, avoiding complications due to contact metamorphism, to derive:

$$\Delta^{13}C\ (Cc\text{-}Gr) = 3.56 \times 10^6 / T^2\ (K) \qquad (10)$$

At high temperatures, >600°C, independent petrologic thermometry is in excellent agreement with this calibration (Table 6) and with that of Chacko et al. (1991, CMCG). The theoretical calculations of Polyakov and Kharlishina (1994, 1995) yield a slightly smaller partition function ratio than used by Chacko et al. (1991) and suggest a small

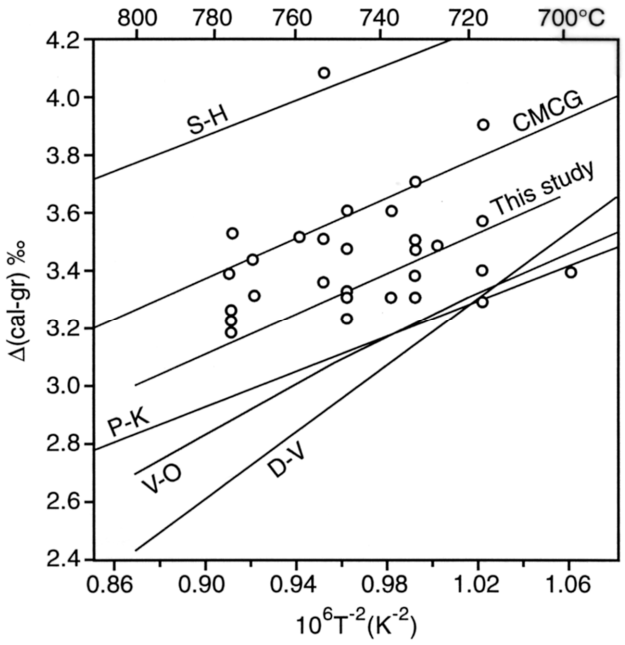

Figure 15. Temperature dependence of $\Delta^{13}C$(Cc-Gr) as determined by various workers: This Study = Kitchen and Valley (1995); CMCG = Chacko et al. (1991); S-H = Scheele and Hoefs (1992); P-K = Polyakov and Kharlishina (1995); D-V = Dunn and Valley (1992); V-O = Valley and O'Neil (1981). Data points are for granulite facies marbles from the Adirondacks that were sampled over 2 km away from contacts with massif-type anorthosite (from Kitchen and Valley 1995).

pressure correction. The effect of these changes is to reduce slightly the CMCG calibration (R Clayton, pers. comm. 9-94). The experimental calibration of Scheele and Hoefs (1992) leads to temperature estimates that are unreasonably high and which would promote wholesale melting in several granulite facies terrains (Morrison and Barth 1993, Kitchen and Valley 1995, Satish-Kumar and Wada 2000, Satish-Kumar 2000).

The empirical calibration of Dunn and Valley (1992) is fit to data including lower temperature amphibolite facies marbles:

$$\Delta^{13}C\ (Cc\text{-}Gr) = 5.81 \times 10^6 / T^2 - 2.61\ (K) \qquad (11)$$

This is a significantly steeper slope that implies curvature at higher temperature in order to pass through the origin (Fig. 15). Agreement is excellent with the other calibrations at 600-700°C, but temperatures from (11) are increasingly higher than those from (10) below 650°C. Several studies at lower temperatures show that petrologic thermometry agrees better with the results of (11) (Wada and Suzuki 1983, Wada et al. 1984, Bergfield et al. 1996). Two interpretations are possible: there is a significant change in slope that is not predicted by theory, or lower temperature samples used for empirical calibration are not fully equilibrated (see, Kitchen and Valley 1995). Isotopic disequilibrium is well known below 500-600°C, so this possibility cannot be discounted. Regardless of whether the Dunn and Valley calibration is a true thermometer based on equilibrium or a pseudo-thermometer that is dependent on reaction kinetics of graphitization, it is the calibration that has yielded the most reasonable temperature estimates below 600°C (Table 6).

Graphite crystallinity and morphology

Graphite can form by a variety of processes. Commonly, graphite in marbles is derived from sedimentary organic matter that has undergone progressive maturation during metamorphism. This process begins with diagenesis and may not be complete until above 500-600°C (see Dunn and Valley 1992). Changes due to maturation include: the coalescence and coarsening of single crystals (flakes) of graphite; decrease in the elemental ratio, (N+H+S)/C; sharpening and shifts of X-ray diffraction peaks; shifts in Raman spectra (Luque et al. 1998), and increased vitrinite reflectance. High resolution transmission electron microscopy reveals that in the final stages of graphitization (400 to

>500°C), crystallinity increases at the atomic-scale from moderately well-organized rims on grains with immature cores to well-organized crystalline flake graphite (Buseck and Huang 1985).

Graphitization in marble is also accompanied by carbon isotope exchange. Carbon diffusion in graphite is very slow (Thrower and Mayer 1978) and T_C » 800°C (Table 3). High T_C is further indicated by isotopically zoned flakes of graphite that were not homogenized by granulite facies metamorphism (Kitchen and Valley 1995, Farquhar et al. 1999, Satish-Kumar et al. 2000). Thus, carbon isotope exchange between graphite and carbonate is sluggish, rate-limited by graphite, and can only occur upon crystallization or recrystallization of graphite. In contrast, carbon diffusion in calcite is relatively rapid. Accordingly, Cc-Gr thermometry should only be attempted with visible flakes of graphite and the presence of growth-zoning within flakes should be evaluated.

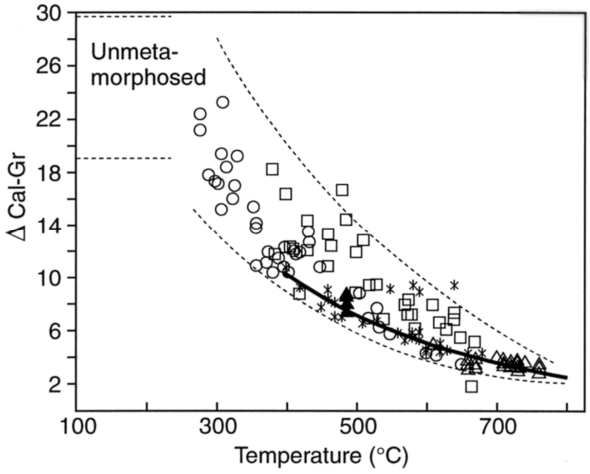

Figure 16. Measured values of Δ(Cc-Gr) versus metamorphic temperature independently determined by petrologic thermometers. Data are from: Valley and O'Neil (1981), open triangles; Wada and Suzuki (1983), asterisks; Kreulen and van Beek (1983), squares; Morikiyo (1984), circles; and Dunn and Valley (1992), solid triangles and heavy curved line. The unmetamorphosed calcite-organic matter fractionation is from Eichmann and Schidlowski (1975). Samples show a successive approach to equilibrium at higher temperatures rate-limited by slow exchange in graphite (from Dunn and Valley 1992).

A number of studies have measured Cc-Gr fractionations that appear too large in relation to equation (10), resulting in temperatures that are lower than expected (Hoefs and Frey 1976, Kreulen and van Beek 1983, Wada and Suzuki 1983, Morikiyo 1984, Wada et al. 1984, Schrauder et al. 1993, Bergfield et al. 1996). These studies support the hypothesis that either the calibration has a steeper slope at low temperatures than is shown in Figure 15 or that the samples are not fully equilibrated. The data in and 17 show that exchange begins at 300°C, but that below 500-600°C, large values of $\Delta^{13}C$(Cc-Gr) are seen that are highly variable indicating incomplete exchange. Equilibration is not assured below 650°C. Dunn and Valley (1992) found that samples with flakes of graphite (vs. less mature carbonaceous material) plot along the bottom of this envelope of fractionations (Fig. 16) and they suggested that the lowest values were equilibrated. Accordingly, the heavy line in Figure 16 is their calibration (Eqn. 11). For these reasons, it is unlikely that values of $\Delta^{13}C$(Cc-Gr) > 8‰ represent equilibrium and values between 5 and 8‰ should be interpreted with extra caution.

Once coarsening and recrystallization stops, graphite flakes will preserve isotope composition due to slow diffusion. Intracrystalline zoning of $\delta^{13}C$ has been detected in some crystals by most studies that have evaluated it. This has been demonstrated by delamination of single flakes at the 20-100 μm-scale (Wada 1988, Arita and Wada 1990, Kitchen and Valley 1995, Satish-Kumar 2000), by ion microprobe (Farquar et al. 1999) or, more simply, by analysis of large vs. small flakes from the same rock (Kitchen and Valley 1995).

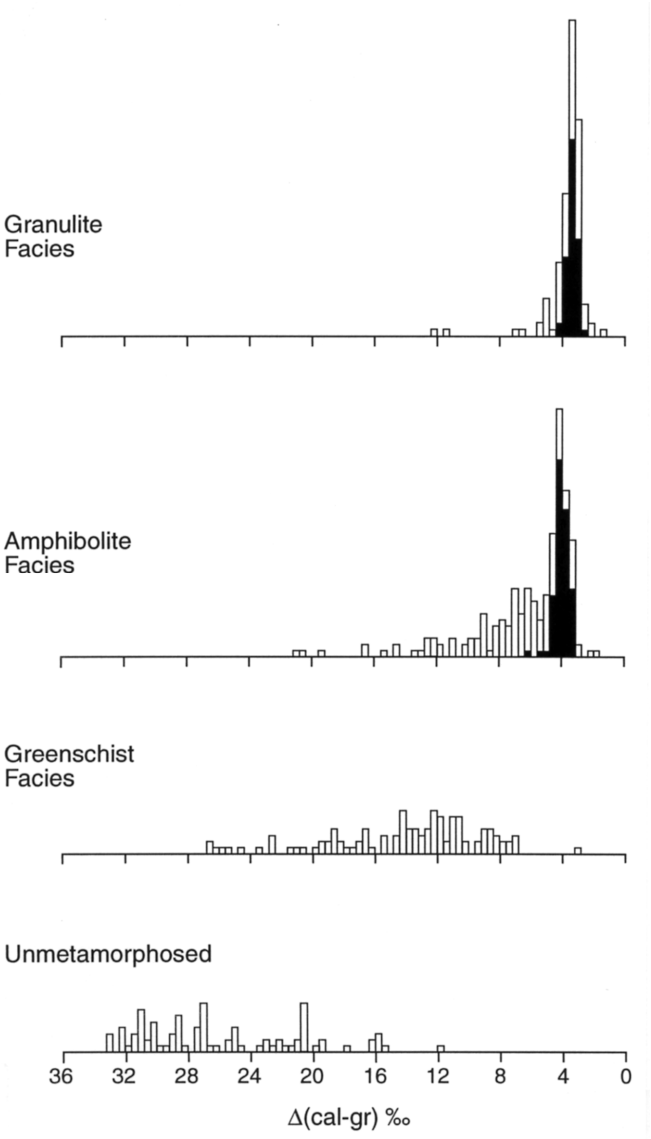

Figure 17. Carbon isotope fractionations as a function of metamorphic grade. (17A) Compilation of measured values of Δ(Cc-Gr) shows scatter and disequilibrium at greenschist facies and lower temperature conditions. Many amphibolite facies and most granulite facies samples show a tight clustering of values consistent with isotope equilibration above 600°C. Values in black are from the Adirondacks (from Kitchen and Valley 1995). (17B) Values of $\delta^{13}C$ for a Liassic black shale formation (Hoefs and Frey 1976) showing successive approach to equilibrium at maximum T = 500-600°C (from Sharp et al. 1995).

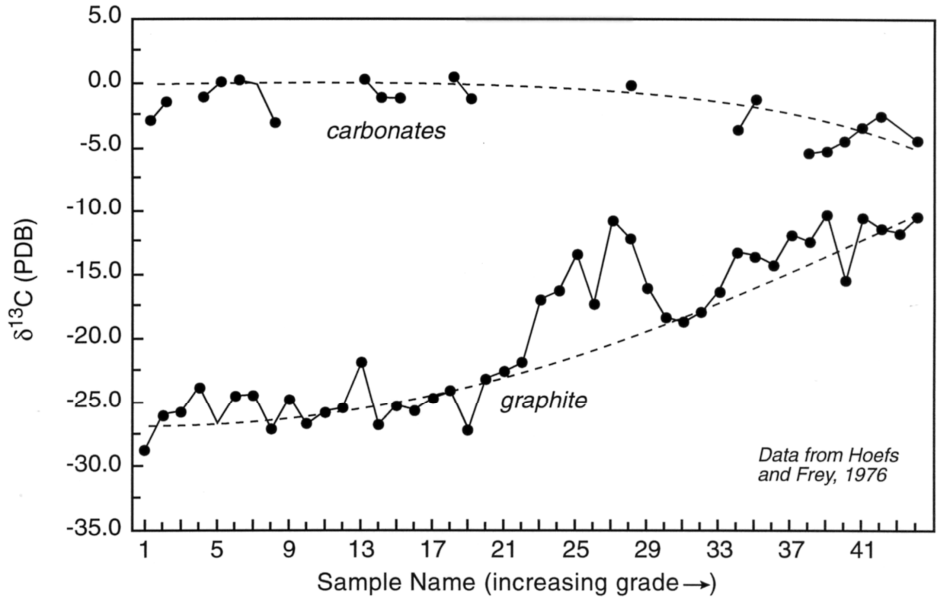

Graphite inclusions wholly within silicate minerals have also been found to have slightly lower $\delta^{13}C$ than graphite in the calcite matrix suggesting that they were armored against prograde exchange (Wada and Suzuki 1983). This effect will not affect thermometry if care is taken to only select graphite that is disaggregated by acid dissolution of carbonate. Conversely, the analysis of selected inclusions from different minerals, or from different positions within a zoned mineral, may provide temperature history of prograde mineral growth.

Skeletal graphite or flakes with etched or pitted surfaces are frequently seen, suggesting retrograde recrystallization. Skeletal graphites with larger $\Delta^{13}C$(Cc-Gr) than metallic flakes support this interpretation (Weis 1980, Arita and Wada 1990). Van der Pluijm and Carlson (1989) determined temperatures were less than 450°C during mylonitization along the Bancroft shear zone in the Grenville Province by reequilibration of $\Delta^{13}C$(Cc-Gr) in 650-700°C marbles. Likewise, graphite spheres with radial texture have been described in nearby marble and Cc-Gr thermometry suggests lower temperature growth (Jaszczak and Robinson 1998; S. Dunn, unpublished 1999). Samples of charnockite from southern India have been shown to contain three generations of graphite varying by up to 10‰ in $\delta^{13}C$ by ion microprobe (Farquhar et al. 1999).

Carbonate/graphite ratio

Accurate thermometry is most likely if the ratio of carbon-in-carbonate to carbon-in-graphite is high. The mode effects on diffusive resetting, described above, are a criterion for RAM thermometry. Also, retrograde precipitation of carbonate is common and may be more significant in carbonate-poor lithologies. Considering the concentration of carbon in each mineral, 100% in graphite vs. 12 wt % in calcite, mode ratios on the order of 100/1 for carbonate/graphite are prudent. This is seldom a concern in marbles where 0.1 to 1.0 vol % graphite is typical, but care should be considered for graphite-rich or carbonate-poor lithologies.

Elsenheimer (1988, 1992) analyzed 11 Cc-Gr pairs from calcite-poor calcsilicates (<3% calcite) in the same region as the 14 marbles reported in Table 6 (#20). The average temperature was the same in each case. However, the marbles yielded a reasonable range from 510 to 740°C while the calcsilicates yielded many unreasonable temperatures from 400 to 1130°C. Likewise, Bergfield et al. (1996) found that Cc-Gr temperatures were lower and more variable in schists than marbles from the Panamint Range. In these two studies, the calcsilicates and schists are graphite-rich and calcite-poor, violating the criteria for a RAM thermometer, and only the temperatures from marble were judged to represent the peak of metamorphism.

Contact and polymetamorphism

There have been a number of applications of Cc-Gr thermometry to contact metamorphism. Wada (1978) studied Cc-Gr pairs in skarns from the Kamioka Mining District and found that graphite in the skarn was similar in $\delta^{13}C$ to that of the country rocks. However skarn calcite was 5-10‰ lower than the equilibrium value with graphite and gradients of up to 10‰/2cm were measured in $\delta^{13}C$(Cc). Wada and Suzuki (1983) found a good correlation of $\Delta^{13}C$(Cc-Gr) and temperature from 400 to 680°C, however, as discussed for (11), it is not certain if this correlation is controlled by equilibrium or kinetics.

Arita and Wada (1990) studied the effects of contact metamorphism overprinted on granulite facies marbles of the Hida belt and found that the cores of graphite and calcite retained granulite facies fractionations, but that profound gradients in composition and disequilibrium existed from core to rim within single crystals.

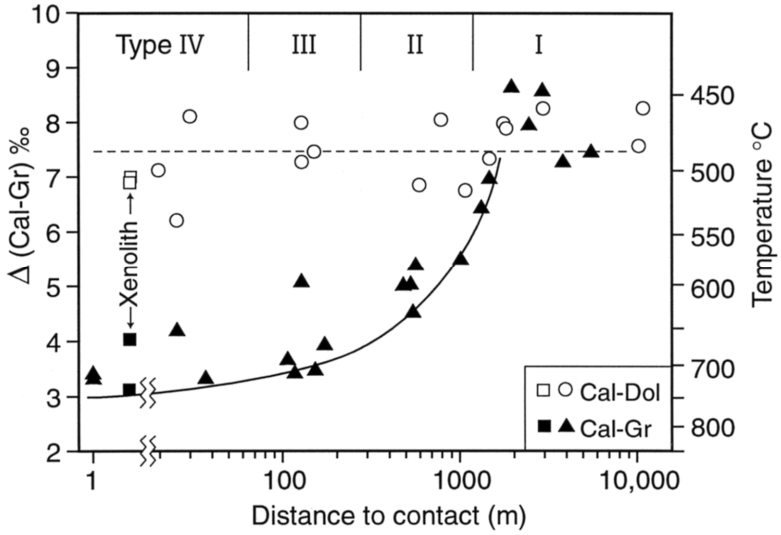

Figure 18. The results of calcite-graphite isotope thermometry (filled symbols) and calcite-dolomite solvus thermometry (open symbols) plotted against distance to the Tudor Gabbro contact, Ontario. The solvus thermometry is reset by regional metamorphism at 490°C while the isotope thermometry preserves high temperatures due to earlier contact metamorphism. The solid curved line is the predicted thermal gradient for contact metamorphism (from Dunn and Valley 1992).

Two studies have demonstrated the preservation of high contact metamorphic temperatures adjacent to mafic plutons in terranes that subsequently experienced lower temperatures during regional metamorphism. Cc-Gr temperatures in marble smoothly increase from 500 to 700°C approaching the Tudor gabbro, Ontario. The increase in temperature correlates with a change from fine grained gray marble to coarser white marble and with mineral isograds (Dunn and Valley 1992, 1996). However, the temperatures recorded by calcite-dolomite solvus thermometry are uniform at 490°C (Fig. 18). Thus, the Cc-Gr thermometer has seen through the regional metamorphic overprint that reequilibrated the Mg content of calcite and dolomite. Kitchen and Valley (1995) delaminated single flakes of graphite in granulite facies marbles from the central Adirondacks and found gradients in $\delta^{13}C$ in crystals from within 10 km (ca. 0-1 km in 3-D) of exposed massif-type anorthosite. The cores of these grains suggest relict temperatures as high as 890°C while the rims record the subsequent regional metamorphism at 700-750°C.

Fluid flow

Calcite-graphite thermometry requires that carbon-bearing fluids have not infiltrated with contrasting $\delta^{13}C$. Conversely, $\Delta^{13}C$(Cc-Gr) can be used to infer fluid flow. Several studies have shown that calcite and/or graphite is zoned in $\delta^{13}C$ (Wada 1988, Arita and Wada 1990, Kitchen and Valley 1995, Satish-Kumar et al. 1998, Farquhar et al. 1999). Most commonly, this results from open system exchange with grain boundary fluids that have also caused a significantly larger zonation in $\delta^{18}O$ (Wada 1988, Graham et al. 1998, Satish-Kumar et al. 1998), indicating that fluids were H_2O rich. Likewise, if temperature is independently known, then discordant or variable Cc-Gr T's may reflect fluid infiltration. Conversely, systematic and self-consistent Cc-Gr thermometry in rocks of variable $\delta^{13}C$ demonstrates that significant amounts of carbon-rich fluid (CO_2 or CH_4) have not pervasively infiltrated large areas of granulite facies terrains (Adirondacks, Anabar Shield, Cucamonga Terrane in San Gabriel Mtns, E. Antarctica, Ivrea Zone, or southern India, see Table 6).

Other minerals

Some studies have included limited analysis of graphite pairs with other carbon-bearing minerals, including dolomite (Wada and Oana 1975, Wada 1977, Wada and Suzuki 1983, Kitchen and Valley 1995, Brady et al. 1998), siderite (Perry and Ahmad 1977), and cordierite (Vry et al. 1988, Fitzsimons and Mattey 1994). Moecher et al. (1992, 1994) estimate that $\Delta^{13}C$(Cc-scapolite) ≅ 0.1‰ in granulites, suggesting that small amounts of scapolite may not adversely affect Cc-Gr thermometry and that scapolite-graphite thermometry is possible in selected rocks.

Biogenic versus abiogenic graphite

The controversy over biogenic vs. abiogenic formation of graphite has a long history and implications for interpreting the earliest record of life on Earth and possibly Mars (Schidlowski 2001), subduction of sediments into the mantle (Kyser 1986, Schulze et al. 1997), and controversy over genesis of fossil fuels (Gold 1987, Valley et al. 1988). While low values of $\delta^{13}C$ are generally accepted as evidence for biogenic origin, this evidence can be obscured by metamorphic exchange in carbonate-bearing rocks. For instance, intermediate values of $\delta^{13}C$(Gr)= -9.3 to -10.7 in 3.8 Ga amphibolite facies meta-sediments from Isua, Greenland are interpreted as abiogenic and in equilibrium with coexisting siderite ($\Delta^{13}C$(Sid-Gr) = 5.8-6.0‰; Perry and Ahmad 1977). Subsequent studies of graphite in rocks that do not contain carbonate from Isua show a range of values to –28‰ that are interpreted as biogenic (Schidlowski et al. 1979, Hayes et al. 1983). These low values have been verified in related rocks by ion microprobe, strengthening the interpretation of earliest life (Mojzsis et al. 1996, Schidlowski 2001).

The initial sedimentary value of $\delta^{13}C$ of carbonaceous matter can be estimated from mass-balance even in marbles that have undergone inter-mineral metamorphic exchange at high temperature. Kitchen and Valley (1995) found a strong inverse correlation of graphite/calcite ratio and $\delta^{13}C$(Gr). They calculated that even though all graphite in their study now has $\delta^{13}C > -10$‰, this value results from metamorphic exchange with calcite. In all rocks, the protolith carbonaceous matter is estimated at $\delta^{13}C < -25$, indicative of a biogenic origin. Likewise, Morrison and Barth (1993) and Bergfield et al. (1996) show that mass-balance and exchange with carbonate controls $\delta^{13}C$(Gr) in marbles.

Adirondack Mountains—A case study

Graphite-bearing calcite marbles are common throughout the upper amphibolite facies NW Adirondack Lowlands and locally in the granulite facies central Adirondack Highlands. Figure 19A shows the results of Cc-Gr thermometry for 89 samples from the NW and 55 from the central Adirondacks (Kitchen and Valley (1995). All graphites were flakes freed by dissolution of carbonate. Five outcrop tests were made and reproducibility of temperatures is ±10-20°C except where calcites are heterogeneous (Table 2).

The 55 granulite facies samples include 17 that are from near the plutonic contacts of massif-type anorthosite bodies. These samples contain zoned graphite crystals with higher $\delta^{13}C$ cores that record the pre-regional metamorphism igneous contact temperatures.

The data for the NW Adirondacks show that the central zone of the region (B in Fig. 19B) experienced systematically lower temperatures, averaging 640°C and that temperatures increase systematically towards transitions to granulite facies conditions to the SE across the Carthage-Colton Line and to the NW across the St. Lawrence River. A temperature of 675°C is recorded for the orthopyroxene isograd to the SE. The two 675°C isotherms parallel the strike of dominant lithologies in the area and are normal to the NW vergence, in good agreement with recent petrologic thermometry (Liogys and

Jenl

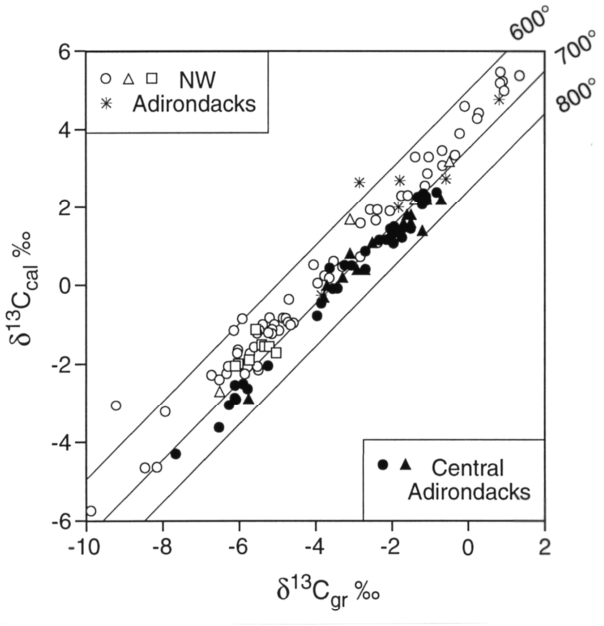

Figure 19. Carbon isotope thermometry for Adirondack marbles. (19A) Plot of δ^{13}C(calcite) vs. δ^{13}C(graphite). Open symbols are for upper the amphibolite facies NW Adirondacks and closed symbols are for the granulite facies Adirondack Highlands. (19B) Values of Δ(Cc-Gr) in per mil and resulting isopleths for 675°C parallel the strike of the terrane and, show lower metamorphic temperatures centered on Gouverneur and increasing towards granulite facies rocks to the SE and to NW. Note outcrop tests at Fish Creek (FC), the Train Wreck (TW) and the Valentine Mine (VM) (from Kitchen and Valley 1995).

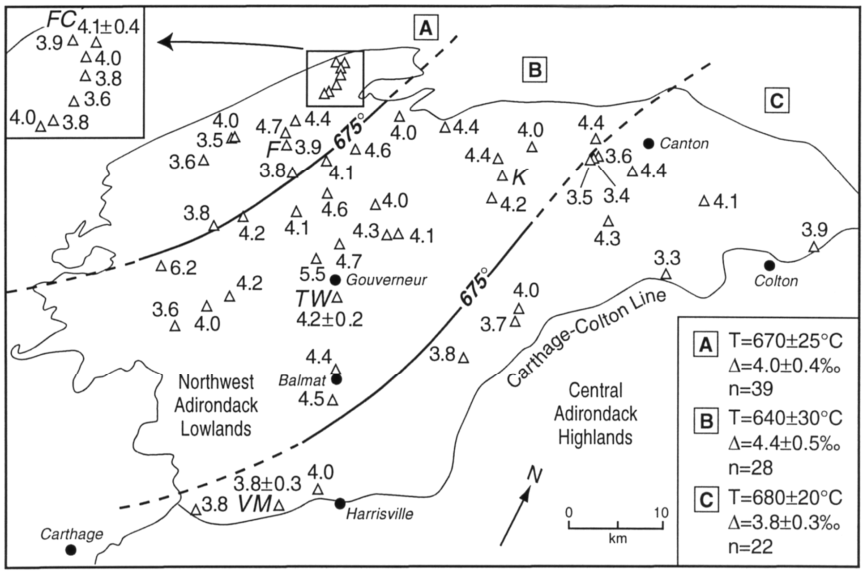

Jenkins 2000). No zones of higher temperature were found at exposed igneous contacts, though the locally low values of Δ^{13}C(Cc-Gr) 5 km W of Canton may be an unrecognized contact aureole. The Cc-Gr RAM thermometer provides the best estimates for metamorphic temperature in this terrane.

SULFUR ISOTOPE THERMOMETRY

Several common sulfide mineral pairs have fractionations that are calibrated and appropriate for thermometry, especially in sulfide deposits. However thermometry has often been disappointing, and sulfur isotope studies have tended to concentrate on elucidating fluid conditions, sources of sulfur, and ore mineral paragenesis (Ohmoto 1986). Recent microanalysis by laser probe and ion microprobe documents one of the main problems. Sulfides forming at low to intermediate temperatures show extreme zonation of δ^{34}S, over 50‰ in less than 100 μm in some diagenetic pyrites (McKibben and Riciputi 1998) and 4-5‰/cm in a hydrothermal black smoker vent (Shanks et al. 1998).

Crowe (1994) analyzed coexisting pyrite-chalcopyrite pairs from the stockwork feeder zones of several volcanogenic massive sulfide deposits. Individual 200-μm diameter grains were analyzed by laser. Sulfides that were in grain to grain contact were found to have exchanged during greenschist to upper amphibolite facies metamorphism and during cooling, while sulfides that were isolated by quartz matrix preserved original hydrothermal $\delta^{34}S$ values. Temperatures of 170-424°C were calculated for three different hydrothermal systems. Thus, reliable thermometry will require assessment of sub-mm scale isotope zonation and exchange kinetics in sulfide minerals.

SKARNS

Skarns and hydrothermal veins associated with shallow igneous activity offer excellent opportunities for stable isotope thermometry because minerals commonly co-precipitate directly from a fluid and cool quickly. Minerals that are not zoned in chemical composition are most promising. Tests can be applied for mineral zoning or precipitation from evolving fluids.

Bowman (1998) reviewed stable isotope studies of skarns (Table 7). In a number of skarns, temperatures are reported that are generally consistent with the results of phase equilibria and fluid inclusion thermometry. However, minerals that have not co-precipitated do not typically yield self-consistent temperature estimates with the different techniques. Stable isotope concordance is also a good test. For instance, quartz, calcite and magnetite appear texturally to be co-precipitated and were analyzed from ten rocks in the Hanover Zn-Pb skarn (Table 7, #8, Turner and Bowman 1993). The Qt-Mt temperatures are in good agreement with independent thermometry, but the Cc-Qt and Cc-Mt temperatures are too low and too high, respectively (Table 7) because of late-stage depletion of $^{18}O/^{16}O$ in calcite (Bowman 1998).

Stable isotope zonation at the cm-scale is well documented in skarns, but few samples have been tested at mm to μm-scale (Jamtveit and Hervig 1994, Bezenek et al. 1995, Clechenko and Valley 2000). A careful study would include petrography and imaging, and other tests of temperature reliability. Microanalysis should be employed when other tests fail. It offers a powerful new tool for resolving the thermal and fluid evolution of skarns.

ONE-MINERAL THERMOMETERS

Isotope fractionation can occur among crystallographically distinct sites within single minerals creating a potential one mineral thermometer. However, techniques for extraction and analysis of the isotope ratio of a specific site vary greatly in difficulty and reliability, and more experimental calibrations of fractionation are needed. Specific studies for oxygen isotopes include: clays (Hamza and Epstein 1980, Bechtel and Hoernes 1990, Sheppard and Gilg 1996); phyllosilicates (Savin and Lee 1988); analcime

NOTES for Table 7 (next page)

[1]Mineral abbreviations: Am = amphibole, Anh = anhydrite, Bt = biotite, Cal = calcite, Ccp = chalcopyrite, Chl = chlorite, Ep = epidote, Grt = garnet, Gn =galena, Hem = hematite, Mag = magnetite, Ms = muscovite, Pl = plagioclase, Px = pyroxene,. Py = pyrite, Qtz = quartz, Sp = sphalerite.

[2]Number of pairs analyzed in parentheses.

[3]Pressure (MPa) used in study for calculating phase equlibria and for correcting fluid-inclusion microthermometry data..

*References: 1. Taylor & O'Neil 1977; 2. Shelton & Rye 1982; Shelton 1983; 3. Bowman et al. 1985a; 4. Jamtveit et al. 1992a,b; 5. Bowman et al. 1985b; 6. Brown et al. 1985; 7. Layne & Spooner 1991; Layne et al. 1991; 8. Turner & Bowman 1993; 9. Kemp 1985; 10. Shimizu & Iiyama 1982.

Table 7. Comparison of temperature estimates (°C) from stable isotopes, phase equilbria, and fluid inclusions in skarns (from Bowman 1998).

			Stage	*Isotope temperature*			*Skarn*	*Type*	*Phase*	*Fluid inclusion*			P_{Corr}
				Ave.	*Max.*	*Min.*	**(reference)*		*equil.*	*Ave.*	*Max.*	*Min.*	*(Mpa)*
	Osgood Mtns., Nevada	W	I	381	640	330	Qtz-Grt (11)	575					150
		Cu, Au	II	523	540	480	Qtz-Am (6)	475					150
				636	1000	505	Qtz-Cal (7)						
2.													
	Mines Gaspe, Quebec	Cu	II	412	552	366	Py-Ccp (6)	500	340	350	425	200	30
			III	688	801	550	Anh-Py, Ccp (20)						
3.													
	Cantung, NWT	W	I	478	500	460	Qtz-Px (6)	575			410	360	100
			II	505	525	485	Qtz-Bt (2)	475			400	350	100
4.													
	Oslo Rift, Norway	W, Zn Cu	II	360	360	360	Qtz-Grt (1)	380		350	400	300	50
5.													
	Elkhorn, Montana	-	I	497	660	420	Pl-Px (11)	560	490				100
6.													
	Pine Creek, California	W	I	494	560	400	Qtz-Px (8)	590					150
7.													
	JC, Yukon	Sn	III	460	504	416	Qtz-Ep (2)	550			500	410	75
			IV	446	446	446	Qtz-Bt (1)	450			560	430	75
			V	441	441	441	Cal-Ms (1)	450					
8.													
	Hanover, New Mexico	Zn, Pb	I	391	405	377	Grt-Mag (2)	425		355	400	305	40
				432	506	337	Cal-Ep,Chl (13)						
				625	1128	353	Qtz-Cal,Ep (9)						
			III	358	483	291	Qtz-Mag (12)	380		315	375	255	40
				172	377	-3	Qtz-Cal (10)	0					
				401	533	336	Cal-Mag (10)						
9.													
	Alta, Utah	Cu	I	538	595	500	Px-Mag (5)	575			>580	380	150
			II		Reversal		Qtz-Cal (5)			395	445	345	150
10.													
	Nakatatsu, Japan	Zn, Pb	II	329	364	278	Sp-Gn (4)	390					30

(Karlsson and Clayton 1990, Cheng et al. 2000); micas and chlorite (Hamza and Epstein 1980); scapolite (Moecher et al. 1984); alunite (Ustinov and Grinenko 1985, O'Neil and Pickthorn 1988, Rye et al. 1992); sahaite and spurrite (Ustinov and Grinenko 1985); and apatites (Shemesh et al. 1983, 1988, Ustinov and Grinenko 1985, Zheng 1996). Such studies hold great promise, especially in sedimentary rocks where co-precipitated minerals are rare.

ACKNOWLEDGMENTS

I thank James R. O'Neil for introducing me to the rigor and the fun of stable isotope geochemistry, and for many years of friendship and inspiration. Much of the research reported here was supported by NSF and DOE. Figures were redrafted by Mary Diman. John Eiler, James Farquhar, Yaron Katzir, William Peck, and Zach Sharp are thanked for helpful reviews.

REFERENCES

Addy SK, Garlick GD (1974) Oxygen isotope fractionation between rutile and water. Contrib Mineral Petrol 45:119-121

Agrinier P (1991) The natural calibration of $^{18}O/^{16}O$ geothermometers: Application to the quartz-rutile mineral pair. Chem Geol 91:49-64

Agrinier P, Javoy M, Smith DC, Pineau F (1985) Carbon and oxygen isotopes in eclogites, amphibolites, veins and marbles from Western Gneiss Region, Norway. Isotope Geosci 52:146-162

Anderson AT (1967) The dimensions of oxygen isotope equilibrium attainment during prograde metamorphism. J Geol 75:323-332

Arita Y, Wada H (1990) Stable isotopic evidence for migration of metamorphic fluids along grain boundaries of marbles. Geochem J 24:173-186

Baker AJ (1988) Stable isotope evidence for limited fluid infiltration of deep crustal rocks from the Ivrea Zone, Italy. Geology 16:492-495

Bechtel Z, Hoernes S (1990) Oxygen isotope fractionation between oxygen of different sites in illite minerals: A potential single-mineral thermometer. Contrib Mineral Petrol 104:463-470

Becker RH, Clayton RN (1976) Oxygen isotope study of a Precambrian banded iron-formation, Hamersley Range, Western Australia. Geochim Cosmochim Acta 40:1153-1165

Bergfeld D, Nabelek PI, Labotka TC (1996) Carbon isotope exchange during polymetamorphism in the Panamint Mountains, California, USA. J Metamor Geol 14:199-212

Bestmann M, Kunze K, Matthews A (2000) The evolution of calcite marble shear zone complex on Thassos island, Greece; Microstructural and textural fabrics and their kinematic significance. J Struc Geol 22:1789-1807

Bezenek SR, Crowe DE, Riciputi LR (1995) Evidence of protracted growth history of skarn garnet using SIMS oxygen isotope, trace element and rare earth element data. Geol Soc Am Abstr Prog 27:67

Bigeleisen J, Mayer MG (1947) Calculation of equilibrium constants for isotopic exchange reactions. J Chem Phys 15:261-267

Bigeleisen J, Perlman ML, Prosser HC (1952) Conversion of hydrogenic materials for isotopic analysis. Analyt Chem 24:1356

Bindeman IN, Valley JW (2000) Formation of low-$\delta^{18}O$ rhyolites after caldera collapse at Yellowstone, Wyoming, USA. Geology 28:719-722

Bindeman IN, Valley JW (2001) Oxygen isotope study of phenocrysts in zoned tuffs and lavas from Timber Mountain/Oasis Valley caldera complex: Generation of large volumes of low-$\delta^{18}O$. Contrib Mineral Petrol (in review)

Bohlen SR, Essene EJ (1977) Feldspar and oxide thermometry of granulites in the Adirondack Highlands. Contrib Mineral Petrol 62:153-169

Bottinga Y, Javoy M (1973) Comments on oxygen isotope geothermometry. Earth Planet Sci Letters 20:250-265

Bottinga Y, Javoy M (1975) Oxygen Isotope Partitioning Among the Minerals in Igneous and Metamorphic Rocks. Rev. Geophys. Space Phys 13:401-418

Bottinga Y, Javoy M (1987) Comments on stable isotope geothermometry: The system quartz-water. Earth Planet Sci Letters 84:406-414

Bowman JR (1998) Stable-Isotope Systematics of Skarns. *In* Lentz DR (ed) Mineral Assoc Canada Short Course Series: Mineralized Intrusion-Related Skarn Systems, p 99-145

Bowman JR, Covert JJ, Clark AH, Mathieson GA (1985a) The Can Tung scheelite skarn orebody, Tungsten, Northwest Territories, Canada: Oxygen, hydrogen and carbon isotope studies. Econ Geol 80:1872-1895

Bowman JR, O'Neil JR, Essene EJ (1985b) Contact skarn formation at Elkhorn Montana. II: Origin and evolution of C-O-H skarn fluids. Am J Sci 285:621-660

Brady JB, Cheney JT, Larson Rhodes A, Vasquez A, Green C, Duvall M, Kogut A, Kaufman L, Kovaric D (1998) Isotope geochemistry of Proterozoic talc occurrences in Archean marbles of the Ruby Mountains, southwest Montana, U.S.A. Geol Materials Res 1:1 [http://www.minsocam.org]

Brown EH, O'Neil JR (1982) Oxygen Isotope Geothermometry and Stability of Lawsonite and Pumpellyite in the Shuksan Suite, North Cascades, Washington. Contrib Mineral Petrol 80:240-244

Brown PE, Bowman JR, Kelly WC (1985) Petrologic and stable isotope constraints on the source and evaluation of skarn-forming fluids at Pine Creek, California. Econ Geol 80:72-95

Buseck PR, Huang BJ (1985) Conversion of carbonaceous material to graphite during metamorphism. Geochim Cosmochim Acta 49:2003-2016

Cartwright I, Valley JW, Hazelwood A (1993) Resetting of oxybarometers and oxygen isotope ratios in granulite facies orthogneisses during cooling and shearing, Adirondack Mountains, New York. Contrib Mineral Petrol 113:208-225

Cavosie AJ, Sharp ZD, Selverstone J (2000) Application of a stable isotope geobarometer: Co-existing aluminosilicates in isotopic equilibrium from the Northern Colorado front range. Geol Soc Am Annual Meeting, p A-115

Cawley JD (1984) Oxygen Diffusion in Alpha Alumina. PhD Thesis, Case Western Reserve University, Cleveland, Ohio

Chacko T, Mayeda TK, Clayton RN, Goldsmith JR (1991) Oxygen and carbon isotope fractionations between CO_2 and calcite. Geochim Cosmochim Acta 55:2867-2882

Chamberlain CP, Conrad ME (1991) The relative permeabilities of quartzites and schists during active metamorphism at mid-crustal levels. Geophys Res Letters 18:959-962

Chamberlain CP, Conrad ME (1992) Oxygen-isotope zoning in garnet: A record of volatile transport. Geochim Cosmochim Acta 57:2613-1619

Chamberlain CP, Ferry JM, Rumble D (1990) The effect of net-transfer reactions on the isotopic composition of minerals. Contrib Mineral Petrol 105:322-336

Cheng X, Zhao P, Stebbins JF (2000) Solid state NMR study of oxygen site exchange and Al-O-Al site concentration in analcime. Am Mineral 85:1030-1037

Chiba H, Chacko T, Clayton RN, Goldsmith JR (1989) Oxygen isotope fractionations involving diopside, forsterite, magnetite, and calcite: Application to geothermometry. Geochim Cosmochim Acta 53:2985-2995

Clayton RN (1981) Isotopic thermometry. *In* Newton RC, Navrotsky A, Wood BJ (ed) Advances in Physical Geochemistry. Springer-Verlag, Berlin, p 85-109

Clayton RN, Epstein S (1958) The relationship between O^{18}/O^{16} ratios in coexisting quartz, carbonate, and iron oxides from various geological deposits. J Geol 66:352-373

Clayton RN, Mayeda TK (1963) The use of bromine pentafluoride in the extraction of oxygen from oxides and silicates for isotopic analysis. Geochim Cosmochim Acta 27:43-52

Clayton RN, Kieffer SW (1991) Oxygen isotopic thermometer calibrations. *In* Taylor HP, O'Neil JR, Kaplan IR (ed) Stable Isotope Geochemistry: A Tribute to Samuel Epstein. Geochem Soc Spec Publ 3:3-10

Clayton RN, Goldsmith JR, Mayeda TK (1989) Oxygen isotope fractionation in quartz, albite, anorthite and calcite. Geochim Cosmochim Acta 53:725-733

Clayton RN, Goldsmith J, Karel KJ, Mayeda T, Newton RC (1975) Limits on the effect of pressure on isotopic fractionation. Geochim Cosmochim Acta 39:1197-1201

Clechenko CC, Valley JW (2000) Oscillatory zoned skarn garnet adjacent to massif anorthosite, Willsboro wollastonite mine, N.E. Adirondack Mts, N.Y. Geol Soc Am Abstr Prog, p A-295

Coghlan RAN (1990) Studies in diffusional transport: Grain boundary transport of O in feldspars, diffusion of O, strontium, and the REEs in garnet and thermal histories of granitic intrusions in south-central Maine using O isotopes. PhD Thesis, Brown University, Providence, Rhode Island

Craig H (1953) The geochemistry of the stable carbon isotopes. Geochim Cosmochim Acta 3:53-92

Crank J (1975) The Mathematics of Diffusion. Clarendon Press, Oxford, UK

Crawford WA, Valley JW (1990) Origin of graphite in the Pickering gneiss and the Franklin marble, Honey Brook Upland, Pennsylvania Piedmont. Geol Soc Am Bull 102:807-811

Criss RE (1999) Principles of Stable Isotope Distribution. Oxford Press, Oxford, UK

Criss RE, Gregory RT, Taylor HP (1987) Kinetic theory of oxygen isotopic exchange between minerals and water. Geochim Cosmochim Acta 51:1099-1108

Crowe DE (1994) Preservation of original hydrothermal $\delta^{34}S$ values in greenschist to upper amphibolite volcanogenic massive sulfide deposits. Geology 22:873-876
Crowe DE, Valley JW, Baker KL (1990) Microanalysis of sulfur isotope zonation by laser microprobe. Geochim Cosmochim Acta 54:2075-2092
Dahl PS (1979) Comparative geothermometry based on major-element and oxygen isotope distributions in Precambrian metamorphic rocks from southwestern Montana. Am Mineral 64:1280-1293
Deines P (1977) On the oxygen isotope distribution among mineral triplets in igneous and metamorphic rocks. Geochim Cosmochim Acta 41:1709-1730
Deloule E, Allegre CJ, Doe B (1986) Lead and sulfur isotope microstratigraphy in galena crystals from Mississippi Valley-type deposits. Econ Geol 81:1307-1321
Deloule E, Albarede F, Sheppard SMF (1991a) Hydrogen isotope heterogeneities in the mantle from ion probe analysis of amphiboles from ultramafic rocks. Earth Planet Sci Letters 105:543-553
Deloule E, France-Lanord C, Albarede F (1991b) D/H analysis of minerals by ion probe. *In* Taylor HP, O'Neil JR, Kaplan IR (eds) Stable Isotope Geochemistry. Geochem Soc Spec Publ 3:53-62
Dennis PF (1984a) Oxygen self-diffusion in quartz under hydrothermal conditions. J Geophys Res 89:4047-4057
Dennis PF (1986) Oxygen self diffusion in quartz. Prog Exp Petrol, NERC Publ D 25:260-265
Des Marais DJ, Moore JG (1984) Carbon and its isotopes in mid-oceanic basaltic glasses. Earth Planet Sci Letters 69:43-57
Desmons J, O'Neil JR (1978) oxygen and hydrogen isotope compositions of eclogites and associated rocks from the eastern Sesia Zone (Western Alps, Italy). Contrib Mineral Petrol 67:79-85
Dodson MH (1973) Closure temperature in cooling geochronological and petrologic systems. Contrib Mineral Petrol 40:259-274
Dodson MH (1979) Theory of cooling ages. *In* Jager E, Hunziker JC (eds) Lectures in Isotope Geology. Springer-Verlag, p 194-202
Doremus RH (1998) Diffusion of water and oxygen in quartz: Reaction-diffusion model. Earth Planet Sci Letters 163:43-51
Dunn SR, Valley JW (1992) Calcite-graphite isotope thermometry: A test for polymetamorphism in marble, Tudor gabbro aureole, Ontario, Canada. J Metamor Geol 10:487-501
Dunn SR, Valley JW (1996) Polymetamorphic fluid-rock interaction of the Tudor Gabbro and adjacent marble, Ontario. Am J Sci 296:244-295
Edwards KJ, Valley JW (1998) Oxygen isotope diffusion and zoning in diopside: The importance of water fugacity during cooling. Geochim Cosmochim Acta 62:2265-2277
Eichmann R, Schidlowski M (1975) Isotopic fractionation between coexisting organic carbon-carbonate pairs in Pre-Cambrian sediments. Geochim Cosmochim Acta 39:585-595
Eiler JM, Valley JW (1994) Preservation of premetamorphic oxygen isotope ratios in granitic orthogneiss from the Adirondack Mountains, New York, USA. Geochim Cosmochim Acta 58:5525-5535
Eiler JM, Baumgartner LP, Valley JW (1992) Intercrystalline stable isotope diffusion: A fast grain boundary model. Contrib Mineral Petrol 112:543-557
Eiler JM, Baumgartner LP, Valley JW (1993) A new look at stable isotope thermometry. Geochim Cosmochim Acta 57:2571-2583
Eiler JM, Baumgartner LP, Valley JW (1994) Fast grain boundary: A Fortran-77 program for calculating the effects of retrograde interdiffusion of stable isotopes. Computers Geosciences 20:1415-1434
Eiler JM, Graham CW, Valley JW (1997a) SIMS analysis of oxygen isotopes: Matrix effects in complex minerals and glasses. Chem Geol 138:221-244
Eiler JM, Valley JW, Graham CM (1997b) Standardization of SIMS analysis of O and C isotope ratios in carbonate from ALH84001. 28th Lunar Planet Sci Conf, p 327-328
Eiler JM, Valley JW, Graham CM, Baumgartner LP (1995a) The oxygen isotope anatomy of a slowly cooled metamorphic rock. Am Mineral 80:757-764
Eiler JM, Valley JW, Graham CM, Baumgartner LP (1995b) Ion microprobe evidence for the mechanisms of stable isotope retrogression in high-grade metamorphic rocks. Contrib Mineral Petrol 18:365-378
Eldridge CS, Compston W, Williams IS, Both RA, Walshe JL, Ohmoto H (1988) Sulfur isotope variability in sediment-hosted massive sulfide deposits as determined using the ion microprobe SHRIMP: I. An example from the Rammelsberg orebody. Econ Geol 83:443-449
Elphick SC, Graham CM (1988) The effect of hydrogen on oxygen diffusion in quartz: Evidence for fast proton transients? Nature 335:243-245
Elphick SC, Graham CM, Dennis PF (1988) An ion probe study of anhydrous oxygen diffusion in anorthite: A comparison with hydrothermal data and some geological implications. Contrib Mineral Petrol 100:490-495
Elsenheimer DW (1988) Petrologic and Stable Isotopic Characteristics of Graphite and Other Carbon-bearing Minerals in Sri Lankan Granulites. MS Thesis, University of Wisconsin, Madison

Elsenheimer DW (1992) Development and Application of Laser Microprobe Techniques for Oxygen Isotope Analysis of Silicates and, Fluid/Rock Interaction During and After Granulite-Facies Metamorphism, Highland Southwestern Complex, Sri Lanka. PhD Thesis, University of Wisconsin, Madison

Elsenheimer DW, Valley JW (1992) *In situ* oxygen isotope analysis of feldspar and quartz by Nd: YAG laser microprobe. Chem Geol Isotope Geosci Section 101:21-42

Elsenheimer DW, Valley JW (1993) Submillimeter scale zonation of $\delta^{18}O$ in quartz and feldspar, Isle of Skye, Scotland. Geochim Cosmochim Acta 57:3669-3676

Esler MB, Griffith DWT, Wilson SR, Steele LP (2000) Precision trace gas analysis by FT-IR spectroscopy. 2. The $^{13}C/^{12}C$ isotope ratio of CO_2. Analyt Chem 72:216-221

Essene EJ (1989) The current status of thermobarometry in metamorphic rocks. *In* Daly JS, Cliff RA, Yardley BWD (eds) Evolution of Metamorpic Belts, p 1-44

Farquhar J, Chacko T (1994) Exsolution-enhanced oxygen exchange: Implications for oxygen isotope closure temperatures in minerals. Geol 22:751-754

Farquhar J, Rumble D (1998) Comparison of oxygen isotope data obtained by laser fluorination of olivine with KrF excimer laser and CO_2 laser. Geochim Cosmochim Acta 62:3141-3149

Farquhar J, Chacko T, Frost BR (1993) Strategies for high-temperature oxygen isotope thermometry: A worked example from the Laramie Anorthosite Complex, Wyoming, USA. Earth Planet Sci Letters 117:407-422

Farquhar J, Chacko T, Ellis DJ (1996) Preservation of oxygen isotope compositions in granulites from Northwestern Canada and Enderby Land, Antarctica: Implications for high-temperature isotopic thermometry. Contrib Mineral Petrol 125:213-224

Farquhar J, Hauri E, Wang J (1999) New insights into carbon fluid chemistry and graphite precipitation: SIMS analysis of granulite facies graphite from Ponmudi, South India. Earth Planet Sci Letters 171:607-621

Farver JR (1989) Oxygen self-diffusion in diopside with application to cooling rate determinations. Earth Planet Sci Letters 92:386-396

Farver JR (1994) Oxygen self-diffusion in calcite: Dependence on temperature and water fugacity. Earth Planet Sci Letters 121:575-587

Farver JR, Giletti BJ (1985) Oxygen diffusion in amphiboles. Geochim Cosmochim Acta 49:1403-1411

Farver JR, Giletti BJ (1989) Oxygen and strontium diffusion kinetics in apatite and potential applications to thermal history determinations. Geochim Cosmochim Acta 53:1621-1631

Farver JR, Yund RA (1990) The effect of hydrogen, oxygen, and water fugacity on oxygen diffusion in alkali feldspar. Geochim Cosmochim Acta 54:2953-2964

Farver JR, Yund RA (1991) Oxygen diffusion in quartz: Dependence on temperature and water fugacity. Chem Geol 90:55-70

Farver JR, Yund RA (1991) Measurement of oxygen grain boundary diffusion in natural, fine-grained, quartz aggregates. Geochim Cosmochim Acta 55:1597-1607

Farver JR, Yund RA (1992) Oxygen diffusion in a fine-grained quartz aggregate with wetted and nonwetted microstructures. J Geophys Res 97:14,017-14,029

Farver JR, Yund RA (1995) Grain boundary diffusion of oxygen, potassium and calcium in natural and hot-pressed feldspar aggregates. Contrib Mineral Petrol 118:340-355

Farver JR, Yund RA (1995) Interphase boundary diffusion of oxygen and potassium in K-feldspar/quartz aggregates. Geochim Cosmochim Acta 59:3697-3705

Farver JR, Yund RA (1998) Oxygen grain boundary diffusion in natural and hot-pressed calcite aggregates. Earth Planet Sci Letters 161:189-200

Farver JR, Yund RA (1999) Oxygen bulk diffusion measurements and TEM characterization of a natural ultramylonite: Implications for fluid transport in mica-bearing rocks. J Metamor Geol 17:669-683

Fiebig J, Wiechert U, Rumble D, Hoefs J (1999) High precision, insitu oxygen isotope analysis of quartz using an ArF laser. Geochim Cosmochim Acta 63:687-702

Fitzsimons ICW, Mattey DP (1994) Carbon isotope constraints on volatile mixing and melt transport in granulite-facies migmatites. Earth Planet Sci Letters 134:319-328

Forester RW, Taylor Jr. HP (1976) ^{18}O depleted igneous rocks from the Tertiary complex of the Isle of Mull, Scotland. Earth Planet Sci Letters 32:11-17

Forester RW, Taylor HP (1977) $^{18}O/^{16}O$, D/H, and $^{13}C/^{12}C$ studies of the Tertiary igneous complex of Skye, Scotland. Am J Sci 277:136-177

Fortier SM, Giletti BJ (1989) An empirical model for predicting diffusion coefficients in silicate minerals. Science 245:1481-1484

Fortier SM, Giletti BJ (1991) Volume self-diffusion of oxygen in biotite, muscovite, and phlogopite micas. Geochim Cosmochim Acta 55:1319-1330

Fortier SM, Luttge A, Satir M, Metz P (1994) Oxygen isotope fractionation between fluorphlogopite and calcite: An experimental investigation of temperature dependence and F^-/OH^- effects. Eur J Mineral 6:53-65

Fourcade S, Javoy M (1973) Rapports $^{18}O/^{16}O$ dans les roches du vieux socle catazonal d'ln Ouzzal (Sahara Algerien). Contrib Mineral Petrol 42:235-244

Freer R, Dennis PF (1982) Oxygen diffusion studies. I. A preliminary ion microprobe investigation of oxygen diffusion in some rock-forming minerals. Mineral Mag 45:179-192

Friedman I, O'Neil JR (1977) Compilation of Stable Isotope Fractionation Factors of Geochemical Interest. U S Geol Surv Prof Paper 440-KK

Galimov EM, Rozen OM, Belomestnykh AV, Zlobin VL, Kromtsov IN (1990) The Nature of Graphite in Anabar-Shield Metamorphic Rocks. Geokhimiya 3:373-384

Gerdes ML, Valley JW (1994) Fluid flow and mass transport at the Valentine wollastonite deposit, Adirondack Mountains, N.Y. J Metamor Geol 12:589-608

Ghent ED, Valley JW (1998) Oxygen isotope study of quartz-Al_2SiO_5 pairs from the Mica Creek area, British Columbia: Implications for the recovery of peak metamorphic temperatures. J Metamor Geol 16:223-230

Giletti BJ (1986) Diffusion effects on oxygen isotope temperature of slowly cooled igneous and metamorphic rocks. Earth Planet Sci Letters 77:218-228

Giletti BJ, Yund RA (1984) Oxygen diffusion in quartz. J Geophys Res 89:4039-4046

Giletti BJ, Hess KC (1988) Oxygen diffusion in magnetite. Earth Plant Sci Letters 89:115-122

Giletti BJ, Semet MP, Yund RA (1978) Studies in diffusion—III. Oxygen in feldspars: An ion microprobe determination. Geochim Cosmochim Acta 42:45-57

Godfrey JD (1962) The deuterium content of hydrous minerals from the East-Central Sierra Nevada and Yosemite National Park. Geochim Cosmochim Acta 26:1215-1245

Gold T (1987) Power from the Earth. Dent & Sons Ltd, London, Melbourne, 208 p

Goldman DS, Albee AL (1977) Correlation of Mg/Fe partitioning between garnet and biotite with $^{18}O/^{18}O$ partitioning between quartz and magnetite. Am J Sci 277:750-767

Graham CM, Valley JW, Winter BL (1996) Ion microprobe analysis of $^{18}O/^{16}O$ in authigenic and detrital quartz in St. Peter sandstone, Michigan Basin and Wisconsin Arch, USA: Contrasting diagenetic histories. Geochim Cosmochim Acta 24:5101-5116

Graham CM, Valley JW, Eiler JM, Wada H (1998) Timescales and mechanisms of fluid infiltration in a marble: An ion microprobe study. Contrib Mineral Petrol 132:371-389

Gregory RT, Criss RE (1986) Isotopic exchange in open and closed systems. Rev Mineral 16:91-127

Gregory RT, Taylor HP (1986a) Possible non-equilibrium oxygen isotope effects in mantle nodules, an alternative to the Kyser-O'Neil-Carmichael $^{18}O/^{16}O$ geothermometer. Contrib Mineral Petrol 93: 114-119

Gregory RT, Taylor HP (1986b) Non-equilibrium, metasomatic $^{18}O/^{16}O$ effects in upper mantle mineral assemblages. Contrib Mineral Petrol 93:124-135

Gregory RT, Criss RE, Taylor HP (1989) Oxygen isotope exchange kinetics of mineral pairs in closed and open systems: Applications to problems of hydrothermal alteration of igneous rocks and Precambrian iron formations. Chem Geol 75:1-42

Hamza MS, Epstein S (1980) Oxygen isotopic fractionation between oxygen of different sites in hydroxyl-bearing silicate minerals. Geochim Cosmochim Acta 44:173-182

Harte B, Otter ML (1992) Carbon isotope measurements on diamonds. Chem Geol 101:177-183

Hayes JM, Kaplan IR, Wedeking KW (1983) Precambrian organic geochemistry: Preservation of the record. *In* Schopf JW (ed) Earth's Earliest Biosphere: Its Origin and Evolution. Princeton University Press, Princeton, NJ, p 93-134

Hervig RL, Williams P, Thomas RM, Schauer SN, Steele IM (1992) Microanalysis of oxygen isotopes in insulators by secondary ion mass spectrometry. Int'l J Mass Spect Ion Proc 120:45-63

Hildreth W, Christiansen RL, O'Neil JR (1984) Catastrophic isotopic modification of rhyolitic magma at times of caldera subsidence, Yellowstone plateau volcanic field. J Geophys Res 89:8339-8369

Hoefs J (1997) Stable Isotope Geochemistry, 4th edn. Springer-Verlag, Berlin, 201 p

Hoefs J, Frey M (1976) The isotopic composition of carbonaceous matter in a metamorphic profile from the Swiss Alps. Geochim Cosmochim Acta 40:945-951

Hoefs J, Muller G, Schuster AK (1982) Polymetamorphic relations in iron ores from the iron quadrangle, brazil: The correlation of oxygen isotope variations with deformation history. Contrib Mineral Petrol 79:241-251

Hoefs J, Mueller G, Schuster KA, Walde D (1987) The Fe-Mn ore deposits of Urucum, Brazil; an oxygen isotope study. Chem Geol, Isotope Geosci Section 65:311-319

Hoernes S, Friedrickson H (1978) Oxygen and hydrogen isotope study of the polymetamorphic area of the Northern Otztal-Stubal Alps. Contrib Mineral Petrol 67:305-315

Hoernes S, Lichtenstein U, van Reenen DD, Mokgatlha K (1995) Whole-rock/mineral O-isotope fractionations as a tool to model fluid-rock interaction in deep seated shear zones of the Southern Marginal Zone of the Limpopo Belt, South Africa. S Afr J Geol 98:488-497

Hoffbauer R, Hoernes S, Fiorentini E (1994) Oxygen isotope thermometry based on a refined increment method and its applications to granulite-grade rocks from Sri Lanka. *In* Raith M, Hoernes S (eds) Tectonic, Metamorphic and Isotopic Evolution of Deep Crustal Rocks, With Special Emphasis on Sri Lanka, p 199-220

Hoffbauer R, Spiering B (1994) Petrologic phase equilibria and stable isotope fractionations of carbonate-silicate parageneses from granulite-grade rocks of Sri Lanka. Precambrian Res 66:325-349

James HL, Clayton RN (1962) Oxygen isotope fractionation in metamorphosed iron formations of the Lake Superior region and in other iron-rich rocks. *In* Petrologic Studies: Buddington Volume. Geol Soc Am, p 217-239

Jamtveit B, Hervig RL (1994) Constraints on transport and kinetics in hydrothermal systems from zoned garnet crystals. Science 263:505-508

Jamtveit B, Bucher-Nurminen K, Stijfhoorn DE (1992a) Contact metamorphism of layered shale carbonate sequences in the Oslo Rift: I. Buffering infiltration and mechanisms of mass transport. J Petrol 33: 377-422

Jamtveit B, Grorud HF, Bucher-Nurminen K (1992b) Contact metamorphism of layered shale - carbonate sequences in the Oslo Rift: II. Migration of isotopic and reaction fronts around cooling plutons. Earth Planet Sci Letts 114:131-148

Jaszczak J, Robinson G (1998) Spherical graphite from Gooderham, Ontario. 17th Int'l Mineral Assoc Meeting, Toronto, Aug 1998 (abstr)

Javoy M (1977) Stable isotopes and geothermometry. J Geol Soc London 133:609-636

Jenkin GRT, Linklater C, Fallick AE (1991) Modeling of mineral $\delta^{18}O$ values in an igneous aureole: Closed-system model predicts apparent open-system $\delta^{18}O$ values. Geology 19:1185-1188

Jenkin GRT, Fallick AE, Farrow CM, Bowes GE (1991) Cool: A Fortran-77 computer program for modeling stable isotopes in cooling closed systems. Computers and Geosciences 17:391-412

Johnson EA, Rossman GR, Valley JW (2000) Correlation between OH content and oxygen isotope diffusion rate in diopsides from the Adirondack Mountains, New York. Geol Soc Am Abstr Progr 32:A-114

Jones AM, Iacumin P, Young ED (1999) High resolution $\delta^{18}O$ analysis of tooth enamel phosphate by isotope ratio monitoring gas chromatography and UV laser fluorination. Chem Geol 153:241-248

Karlsson HR, Clayton RN (1990) Oxygen and hydrogen isotope geochemistry of zeolites. Geochim Cosmochim Acta 54:1369-1386

Kawabe I (1978) Calculation of oxygen isotope fractionation in quartz-water system with special reference to the low temperature fractionation. Geochim Cosmochim Acta 42:613-621

Kelley SP, Fallick AE (1990) High precision spatially resolved analysis of $\delta^{34}S$ in sulphides using a laser extraction technique. Geochim Cosmochim Acta 54:883-888

Kemp WM (1985) A Stable Isotope and Fluid Inclusion Study of the Contact Al(Fe)-Ca-Mg-Si Skarns in the Alta Stock Aureole, Alta, Utah. MS Thesis, University of Utah, Provo

Kerrich R, Beckinsale RD, Durham JJ (1977) The transition between deformation regimes dominated by intercrystalline diffusion and intracrystalline creep evaluated by oxygen isotope thermometry. Tectonophysics 38:241-257

Kerstel ERT, van Trigt R, Dam N, Reuss J, Meijer HAJ (1999) Simultaneous determination of the $^{2}H/^{1}H$, $^{17}O/^{16}O$, and $^{18}O/^{16}O$ isotope abundance ratios in water by means of laser spectrometry. Analyt Chem 71:5297-5303

King EM, Valley JW, Davis DW, Edwards G (1998) Oxygen isotope ratios of Archean plutonic zircons from granite-greenstone belts of the Superior Province: Indicator of magmatic source. Precambrian Res 92:47-67

King EM, Valley JW, Davis DW, Kowallis BJ (2001) Empirical determination of oxygen isotope fractionation factors for titanite with respect to zircon and quartz. Geochim Cosmochim Acta, in press

Kitchen NE, Valley JW (1995) Carbon isotope thermometry in marbles of the Adirondack Mountains, New York. J Metamor Geol 13:577-594

Knauth LP, Lowe DR (1978) Oxygen isotope geochemistry of cherts from the Onverwacht group (3.4 billion years), Transvaal, South Africa, with implications for secular variations in the isotopic composition of cherts. Earth Planet Sci Letters 41:209-222

Kohn MJ (1999) Why most "dry" rocks should cool "wet." Am Mineral 84:570-580

Kohn MJ, Valley JW (1994) Oxygen isotope constraints on metamorphic fluid flow, Townshend Dam, Vermont, USA. Geochim Cosmochim Acta 58:5551-5566

Kohn MJ, Valley JW (1998) Obtaining equilibrium oxygen isotope fractionations from rocks: Theory and examples. Contrib Mineral Petrol 132:209-224

Kohn MJ, Schoeninger MJ, Valley JW (1996) Herbivore tooth oxygen isotope compositions: Effects of diet and physiology. Geochim Cosmochim Acta 60:3889-3896
Kohn MJ, Spear FS, Valley JW (1997) Dehydration-melting and fluid recycling during metamorphism: Rangeley Formation, New Hampshire, USA. J Petrol 9:1255-1277
Kohn MJ, Valley JW, Elsenheimer D, Spicuzza M (1993) Oxygen isotope zoning in garnet and staurolite: Evidence for closed system mineral growth during regional metamorphism. Am Mineral 78:988-1001
Kreulen R, van Beek PCJM (1983) The calcite-graphite isotope thermometer; data on graphite bearing marbles from Naxos, Greece. Geochim Cosmochim Acta 47:1527-1530
Kronenberg AK, Yund RA, Giletti BJ (1984) Carbon and oxygen diffusion in calcite: Effects of Mn content and PH_2O. Phys Chem Minerals 11:101-112
Krylov DP, Mineev, S.D. (1994) The concept of model-temperature in oxygen isotope geochemistry: An example of a single outcrop from the Rayner Complex (Enderby Land, East Antarctica). Geochim Cosmochim Acta 58:4465-4473
Kyser TK (1986) Stable isotope variations in the mantle. Rev Mineral 16:141-164
Labotka TC, Cole DR, Riciputi LR (2000) Diffusion of C and O in calcite at 100 MPa. Am Mineral 85:488-494
Larson TE, Sharp ZD (2000) Isotopic disequilibrium in the classic triple point localities of New Mexico. Geol Soc Am Annual Meeting, p A-297
Lasaga AC (1998) Kinetic Theory in the Earth Sciences. Princeton University Press, Princeton, New Jersey, 811 p
Layne GD, Longstaffe FJ, Spooner ETC (1991) The JC tin skarn deposit, southern Yukon Territory: II. A carbon, oxygen, hydrogen, and sulfur stable isotope study. Econ Geol 86:48-65
Layne GD, Spooner ETC (1991) The JC tin skarn deposit, southern Yukon Territory: I. Geology, paragenesis, and fluid inclusion microthermometry. Econ Geol 86:29-47
Li H, Schwarcz HP, Shaw DM (1991) Deep crustal oxygen isotope variations: The Wawa-Kapuskasing crustal transect, Ontario. Contrib Mineral Petrol 107:448-458
Liogys VA, Jenkins DM (2000) Hornblende geothermometry of amphibolite layers of the Popple Hill gneiss, north-west Adirondack Lowlands, New York, USA. J Metamor Geol 18:513-530
Loucks RR (1996) Restoration of the elemental and stable-isotopic compositions of diffusionally altered minerals in slowly cooled rocks. Contrib Mineral Petrol 124:346-358
Luque FJ, Pasteris JD, Wopenka B, Rodas M, Barrenechea JF (1998) Natural fluid-deposited graphite: Mineralogical characteristics and mechanisms of formation. Am J Sci 298:471-498
Luz B, Barkan E, Bender ML, Thiemens MH, Boering KA (1999) Triple-isotope composition of atmospheric oxygen as a tracer of biosphere productivity. Nature 400:547-550
Manning JR (1974) Diffusion kinetics and mechanisms in simple crystals. *In* Hofmann AW et al. (eds) Geochemical Transport and Kinetics. Carnegie Inst Washington, Washington, DC, p 3-13
Matthews A (1994) Oxygen isotope geothermometers for metamorphic rocks. J Metamor Geol 12:211-219
Matthews A, Schliestedt M (1984) Evolution of the blueschist and greenschist facies rocks of Sifnos, Cyclades, Greece. Contrib Mineral Petrol 88:150-163
Matthews A, Beckinsale RD, Durham JJ (1979) Oxygen isotope fractionation between rutile and water and geothermometry of metamorphic eclogites. Mineral Mag 43:406-413
McConnell JDC (1995) The role of water in oxygen isotope exchange in quartz. Earth Planet Sci Letters 136:97-107
McCrea JM (1950) On the isotopic chemistry of carbonates and a paleotemperature scale. J Chem Phys 18:849-857
McKibben MA, Riciputi LR (1998) Sulfur Isotopes by Ion Microprobe. *In* McKibben MA, Shanks III WC, Ridley WI (eds) Applications of Microanalytical Techniques to Understanding Mineralizing Processes. Soc Econ Geol Rev Econ Geol 7:121-140
McLelland J, Chiarenzelli J, Perham A (1992) Age, field, and petrological relationships of the Hyde School gneiss, Adirondack Lowlands, New York: Criteria for an intrusive igneous origin. J Geol 100:69-90
Merritt DH, Hayes JM (1994) Factors controlling precision and accuracy in isotope-ratio-monitoring mass spectrometry. Analyt Chem 66:2336-2347
Moecher DP, Sharp ZD (1999) Comparison of conventional and garnet-aluminosilicate-quartz O isotope thermometry: Insights for mineral equilibrium in metamorphic rocks. Am Mineral 84:1287-1303
Moecher DP, Essene EJ, Valley JW (1992) Stable isotopic and petrological constraints on scapolitization of the Whitestone meta-anorthosite, Grenville, Province, Ontario. J Metamor Geol 10:745-762
Moecher DP, Valley JW, Essene EJ (1994) Extraction and carbon isotope analysis of CO_2 from scapolite in deep crustal granulites and xenoliths. Geochim Cosmochim Acta 58:959-967
Mojzsis SJ, Arrhenius G, McKeegan KD, Harrison TM, Nutman AP, Friend RL (1996) Evidence for life on Earth before 3800 million years ago. Nature 384:55-59

Moore DK, Cherniak DJ, Watson EB (1998) Oxygen diffusion in rutile from 750 to 1000 C and 0.1 to 1000 MPa. Am Mineral 83:700-711

Morikiyo T (1984) Carbon isotopic study on coexisting calcite and graphite in the Ryoke metamorphic rocks, northern Kiso district, central Japan. Contrib Mineral Petrol 87:251-259

Morishita Y, Giletti BJ, Farver JR (1996) Volume self-diffusion of oxygen in titanite. Geochem J 30:71-79

Morrison J, Valley JW (1991) Retrograde fluids in granulites: Stable isotope evidence of fluid migration. J Geol 99:559-570

Morrison J, Barth AP (1993) Empirical tests of carbon isotope thermometry in granulites from southern California. J Metamor Geol 11:789-800

Morrison J, Anderson JL (1998) Footwall refrigeration along a detachment fault: Implications for the thermal evolution of core complexes. Science 279:63-66

Muller G, Schuster A, Hoefs J (1986a) The metamorphic grade of banded iron-formations: Oxygen isotope and petrological constraints. Fortschr Mineral 64:163-185

Muller G, Hans-Joachim L, Hoefs J (1986b) Sauerstoff- und Kohlenstoff-Isotopenuntersuchungen an Mineralen aus gebanderten Eisenerzen und metamorphen Gesteinen nordostlich des Eisernen Vierecks in Brasilien. Geologische Jahrb D 79:21-40

Murphey BF, Nier AO (1941) Variations in the relative abundance of the carbon isotopes. Phys Rev 59:771-772

Nagy KL, Giletti BJ (1986) Grain boundary diffusion of oxygen in a macroperthitic feldspar. Geochim Cosmochim Acta 50:1151-1158

Nier AO (1947) A mass spectrometer for isotope and gas analysis. Rev Sci Instr 18:398

O'Hara KD, Sharp ZD, Moecher DP, Jenkin GRT (1997) The effect of deformation on oxygen isotope exchange in quartz and feldspar and the significance of isotopic temperatures in mylonites. J Geol 103:193-204

O'Neil JR (1986) Theoretical and experimental aspects of isotopic fractionation. Rev Mineral 16:1-41

O'Neil JR, Clayton RN (1964) Oxygen isotope geothermometry. *In* Craig H, Miller SL, Wasserburg GJ (eds) Isotope and Cosmic Chemistry, p 148-157

O'Neil JR, Pickthorn WJ (1988) Single mineral oxygen isotope thermometry. Chem Geol 71:369

Ohmoto H (1986) Stable isotope geochemistry of ore deposits. Rev Mineral 16:491-556

Pandey UK, Chabria T, Krishnamurthy P, Viswanathan R, Kumar B (2000) Carbon isotope and X-ray diffraction studies on calcite-graphite system in calc-granulites around Usilampatti Area, Madurai, Tamil Nadu. J Geol Soc India 55:37-46

Patterson WP, Smith GR, Lohmann KC (1993) Continental Paleothermometry and Seasonality Using the Isotopic Composition of Aragonitic Otoliths of Freshwater Fishes. *In* Swart PK, Lohmann KC, McKenzie J, Savin S (eds) Climate Change in Continental Isotopic Records. Geophysical Monogr, p 191-202

Peck WH (2000) Oxygen isotope studies of Grenville Metamorphism and Magmatism. PhD Thesis, University of Wisconsin, Madison

Peck WH, Valley JW, Graham CM (2001) Slow oxygen diffusion in igneous zircons from metamorphic rocks (in review)

Perry EC, Bonnichsen B (1966) Quartz and magnetite oxygen-18–oxygen-16 fractionation in metamorphosed Biwabik Iron Formation. Science 153:528-529

Perry EC, Ahmad SN (1977) Carbon isotope composition of graphite and carbonate minerals from 3.8-AE metamorphosed sediments, Isukasia, Greenland. Earth Planet Sci Letters 36:280-284

Perry EC, Ahmad SN (1981) Oxygen and carbon isotope geochemistry of the Krivoy Rog iron formation, Ukranian SSR. Lithos 14:83-92

Perry EC, Tan FC, Morey GB (1973) Geology and Stable Isotope Geochemistry of the Biwabik Iron Formation, Northern Minnesota. Econ Geol 68:1110-1123

Perry EC, Ahmad SN, Swulius TM (1978) The oxygen isotope composition of 3,800 M.Y. old metamorphosed chert and iron formation from Isukasia, West Greenland. J Geol 86:223-239

Pineau F, Latouche L, Javoy M (1976) L'origine du graphite et les fractionnements isotopiques du carbone dans les marbres metamorphiques des Gour Oumelalen (Ahaggar, Algerie), des Adirondacks (New Jersey, U.S.A.), et du Damara (Namibie, Sud-Ouest africain). Bull Soc Geol France 7 t. XVIII: 1713-1723

Polyakov VB, Kharlashina NN (1994) Effect of pressure on equilibrium isotopic fractionation. Geochim Cosmochim Acta 58:4739-4750

Polyakov VB, Kharlashina NN (1995) The use of heat capacity data to calculate isotope fractionation between graphite, diamond, and carbon dioxide: A new approach. Geochim Cosmochim Acta 59:2561-2572

Putlitz B, Valley JW, Matthews A (2001) Oxygen isotope thermometry of quartz-Al_2SiO_5 veins in high grade metamorphic rocks on Naxos. Contrib Mineral Petrol (in press)

Rafter TA (1957) Sulphur isotopic variations in nature: Part I. The preparation of sulphur dioxide for mass spectrometer examination. New Zealand J Sci Techn B38:849

Rathmell MA, Streepey M, M., Essene EJ, van der Pluijm BA (1999) Comparison of garnet-biotite, calcite-graphite, and calcite-dolomite thermometry in the Grenville Orogen; Ontario, Canada. Contrib Mineral Petrol 134:217-231

Rees CE (1978) Sulphur isotope measurements using SO_2 and SF_6. Geochim Cosmochim Acta 42:383-389

Riciputi LR (1996) A comparison of extreme energy filtering and high mass resolution techniques for measurement of $^{34}S/^{32}S$ ratios by ion microprobe. Rapid Comm Mass Spectrom 10:282-286

Robinson BW, Kusakabe M (1975) Quantitative preparation of sulphur dioxide for $^{34}S/^{32}S$ analyses from sulphides by combustion with cuprous oxide. Analyt Chem 47:1179

Rosenbaum J, Sheppard SMF (1986) An isotopic study of siderites, dolomites and ankerites at high temperatures. Geochim Cosmochim Acta 50:1147-1150

Rosenbaum JM, Mattey D (1995) Equilibrium garnet-calcite oxygen isotope fractionation. Geochim Cosmochim Acta 59:2839-2842

Rumble D (1978) Mineralogy, petrology, and oxygen isotopic geochemistry of the Clough Formation, Black Mountain, Western New Hampshire, U.S.A. J Petrol 19:317-340

Rumble D, Sharp ZD (1998) Laser microanalysis of silicates for $^{18}O/^{17}O/^{16}O$ and of carbonates for $^{18}O/^{16}O$ and $^{13}C/^{12}C$ ratios. *In* McKibben MA, Shanks III WC, Ridley WI (eds) Soc Econ Geol Rev Econ Geol 7:99-119

Rumble D, Yui T-F (1998) The Qinglongshan oxygen and hydrogen isotope anomaly near Donghai in Jiangsu Province, China. Geochim Cosmochim Acta 62:3307-3321

Rye RO, Bethke PM, Wasserman MD (1992) The stable isotope geochemistry of acid sulfate alteration. Econ Geol 87:225-262

Ryerson FJ, McKeegan KD (1994) Determination of oxygen self-diffusion in akermanite, anorthite, diopside, and spinel: Implications for oxygen isotopic anomalies and the thermal histories of Ca-Al-rich inclusions. Geochim Cosmochim Acta 58:3713-3734

Santosh M, Wada H (1993) A carbon isotope study of graphites from the Kerala Khondalite Belt, Southern India: Evidence for CO_2 infiltration in granulites. J Geol 101:643-651

Satish-Kumar M (2000) Ultrahigh-temperature metamorphism in Madurai granulites, Southern India: Evidence from carbon isotope thermometry. J Geol 108:479-486

Satish-Kumar M, Wada H (2000) Carbon isotopic equilibrium between calcite and graphite in Skallen Marbles, East Antarctica: Evidence for the preservation of peak metamorphic temperatures. Chem Geol 166:173-182

Satish-Kumar M, Santosh M, Wada H (1997) Carbon isotope thermometry in marbles of Ambasamudram, Kerala Khondalite Belt, southern India. J Geol Soc India 49:523-532

Satish-Kumar M, Yoshida M, Wada H, Niitsuma N, Santosh M (1998) Fluid flow along microfractures in calcite from a marble from East Antarctica: Evidence from gigantic oxygen isotopic zonation. Geology 26:251-254

Savin SM, Lee M (1988) Isotopic studies of phyllosilicates. Rev Mineral 19:189-223

Scheele N, Hoefs J (1992) Carbon isotope fractionation between calcite, graphite and CO_2: An experimental study. Contrib Mineral Petrol 112:35-45

Schidlowski M (2001) Carbon isotopes as biogeochemical recorders of life over 3.8 Ga of Earth history: Evolution of a concept. Precambrian Res 106:117-134

Schidlowski M, Appel PWU, Eichmann R, Junge CE (1979) Carbon isotope geochemistry of the 3.7×10^9 yr. old Isua sediments, West Greenland: Implications for the Archaean carbon and oxygen cycles. Geochim Cosmochim Acta 43:189-199

Schrauder M, Beran A, Hoernes S, Richter W (1993) Constraints on the Origin and the Genesis of Graphite-Bearing Rocks from the Variegated Sequence of the Bohemian Massif (Austria). Mineral Petrol 49:175-188

Schulze DJ, Valley JW, Viljoen KS, Stiefenhofer J, Spicuzza M (1997) Carbon isotope composition of graphite in mantle eclogites. J Geol 105:379-386

Schwarcz HP (1966) Oxygen isotope fractionation between host and exsolved phases in perthite. Geol Soc Am Bull 77:879-882

Schwarcz HP, Clayton RN, Mayeda T (1970) Oxygen isotopic studies of calcareous and pelitic metamorphic rocks, New England. Geol Soc Am Bull 81:2299-2316

Shanks WC, Crowe DE, Johnson C (1998) Sulfur isotope analyses using the laser microprobe. *In* McKibben RA, Shanks WC, Ridley WI (eds) Soc Econ Geol Rev Econ Geol 7:141-153

Sharma T, Clayton RN (1965) Measurement of O^{18}/O^{16} ratios of total oxygen of carbonates. Geochim Cosmochim Acta 29:1347-1353

Sharp ZD (1990) A laser-based microanalytical method for the *in situ* determination of oxygen isotope ratios of silicates and oxides. Geochim Cosmochim Acta 54:1353-1357

Sharp ZD (1991) Determination of oxygen diffusion rates in magnetite from natural isotopic variations. Geology 19:653-656
Sharp ZD (1992) *In situ* laser microprobe techniques for stable isotope analysis. Chem Geol 101:3-19
Sharp ZD (1995) Oxygen isotope geochemistry of the Al_2SiO_5 polymorphs. Am J Sci 295:1058-1076
Sharp ZD, Essene EJ (1991) Metamorphic conditions of an Archean core complex in the northern Wind River Range, Wyoming. J Petrol 32:241-273
Sharp ZD, Jenkin GRT (1994) An empirical estimate of the diffusion rate of oxygen in diopside. J Metamor Geol 12:89-97
Sharp ZD, Cerling TE (1996) A laser GC-IRMS techniques for *in situ* stable isotope analyses of carbonates and phosphates. Geochim Cosmochim Acta 60:2909-2916
Sharp ZD, Giletti, BJ, Yoder HS (1991) Oxygen diffusion rates in quartz exchanged with CO_2. Earth Planet Sci Letters 107:339-348.
Sharp ZD, Essene EJ, Smyth JR (1993) Ultra-high temperatures from oxygen isotope thermometry of a coesite-sanidine grospydite. Contrib Mineral Petrol 112:358-370
Sharp ZD, Essene EJ, Hunziker JC (1993) Stable isotope geochemistry and phase equilibria of coesite-bearing whiteschists, Dora Maira Massif, western Alps. Contrib Mineral Petrol 114:1-12
Sharp ZD, Frey M, Levi KJT (1995) Stable isotope variations (H, C, O) in a prograde metamorphic Triassic red bed formation, Central Swiss Alps. Schweiz mineral petrogr Mitt 75:147-161
Sharp ZD, O'Neil JR, Essene EJ (1988) Oxygen isotope variations in granulite-grade iron formations: Constraints on oxygen diffusion and retrograde isotopic exchange. Contrib Mineral Petrol 98:490-501
Shelton KL (1983) Composition and origin of ore-forming fluids in a carbonate-hosted porphyry copper and skarn deposit: A fluid inclusion and stable isotope study of Mines Gaspe, Quebec. Econ Geol 78:387-421
Shelton KL, Rye DM (1982) Sulfur isotopic compositions of ores from Mines Gaspe, Quebec: An example of sulfate-sulfide isotopic disequilibria in ore-forming fluids with applications to other porphyry-type deposits. Econ Geol 77:1688-1709
Shemesh A, Kolodny Y, Luz B (1983) Oxygen isotope variations in phosphate of biogenic apatites, II: Phosphorite rocks. Earth Planet Sci Letters 64:405-416
Shemesh A, Kolodny Y, Luz B (1988) Isotope geochemistry of oxygen and carbon in phosphate and carbonate of phosphorite francolite. Geochim Cosmochim Acta 52:2565-2572
Sheppard SMF, Gilg HA (1996) Stable isotope geochemistry of clay minerals. Clay Minerals 31:1-24
Shieh Y-S, Schwarcz HP (1974) Oxygen isotope studies of granite and migmatite, Grenville province of Ontario, Canada. Geochim Cosmochim Acta 38:21-45
Shieh Y-S, Schwarcz HP, Shaw DM (1976) An Oxygen Isotope Study of the Loon Lake Pluton and the Apsley Gneiss, Ontario. Contrib Mineral Petrol 54:1-16
Shimizu M, IIyama JT (1982) Zinc-lead skarn deposits of the Nakatatsu mine, central Japan. Econ Geol 77:1000-1012
Sitzman SD, Banfield JF, Valley JW (2000) Microstructural characterization of metamorphic magnetite crystals with implications for oxygen isotope distribution. Am Mineral 85:14-21
Smalley PC, Stijfhoorn DE, Raheim JH, Dickson JAD (1989) The laser microprobe and its application to the study of C and O isotopes in calcite and aragonite. Sedimentary Geol 65:1-11
Spear FS, Florence FP (1992) Thermobarometry in granulites: Pitfalls and new approaches. Precambrian Res 55:209-241
Stern MJ, Spindel W, Monse EU (1968) Temperature dependence of isotope effects. J Chem Phys 48:2908-2919
Stoffregen RE, Rye RO, Wasserman MD (1994) Experimental studies of alunite: I, ^{18}O-^{16}O and D-H fractionation factors between alunite and water at 250-450°C. Geochim Cosmochim Acta 58:903-916
Taylor BE, O'Neil JR (1977) Stable isotope studies of metasomatic Ca-Fe-Al-Si skarns and associated metamorphic and igneous rocks, Osgood Mountains, Nevada. Contrib Mineral Petrol 63:1-49
Tennie A, Hoffbauer R, Hoernes S (1998) The oxygen isotope fractionation behavior of kyanite in experiment and in nature. Contrib Mineral Petrol 133:346-355
Thrower PA, Mayer RM (1978) Point defects and self-diffusion in graphite. Physica Status Solidi 47:11-37
Turner DR, Bowman JR (1993) Origin and evolution of skarn fluids, Empire zinc skarns, Central Mining District, New Mexico, USA. Appl Geochem 8:9-36
Urey HC (1947) The thermodynamic properties of isotopic substances. J Chem Soc (1947):562-581
Ustinov VI, Grinenko VA (1985) Intrastructural isotope distribution during mineral formation. Geochem Int'l 22:143-149
Valley JW, O'Neil JR (1980) $^{13}C/^{12}C$ exchange between calcite and graphite: A possible thermometer in Grenville marbles. Geochim Cosmochim Acta 45:411-419
Valley JW, Graham CM (1991) Ion microprobe analysis of oxygen isotope ratios in granulite facies magnetites: Diffusive exchange as a guide to cooling history. Contrib Mineral Petrol 109:38-52

Valley JW, Graham CM (1993) Cryptic grain-scale heterogeneity of oxygen isotope ratios in metamorpic magnetite. Science 259:1729-1733

Valley JW, Graham CM (1996) Ion microprobe analysis of oxygen isotope ratios in quartz from Skye granite: Healed micro-cracks, fluid flow, and hydrothermal exchange. Contrib Mineral Petrol 124:225-234

Valley JW, Chiarenzelli J, McLelland JM (1994) Oxygen isotope geochemistry of zircon. Earth Planet Sci Letters 126:187-206

Valley JW, Kinny PD, Schulze MJ (1998b) Zircon megacrysts from kimberlite: Oxygen isotope heterogeneity in mantle melts. Contrib Mineral Petrol 133:1-11

Valley JW, Kitchen N, Kohn MJ, Niendorf CR, Spicuzza MJ (1995) UWG-2, a garnet standard for oxygen isotope ratio: Strategies for high precision and accuracy with laser heating. Geochim Cosmochim Acta 59:5223-5231

Valley JW, Graham CM, Harte B, Eiler JM, Kinny PD (1998a) Ion Microprobe Analysis of Oxygen, Carbon, and Hydrogen Isotope Ratios. *In* McKibben MA, Shanks III WC, Ridley WI (eds) Applications of Microanalytical Techniques to Understanding Mineralizing Processes. Soc Econ Geol Rev Econ Geol 7:73-98

Valley JW, Komor SC, Baker K, Jeffrey AWA, Kaplan IR, Raheim A (1988) Calcite crack cements in granite from the Siljan Ring, Sweden: Stable isotopic results. *In* Boden A, Eriksson KG (eds) Deep Drilling in Crystalline Bedrock. Springer-Verlag, New York, p 156-179

van der Pluijm BA, Carlson KA (1989) Extension in the central metasedimentary belt of the Ontario Grenville: Timing and tectonic significance. Geology 17:161-164

van Haren JLM, Ague JJ, Rye DM (1996) Oxygen isotope record of fluid infiltration and mass transfer during regional metamorphism of pelitic schist, Connecticut, USA. Geochim Cosmochim Acta 60:3487-3504

Vannay J-C, Sharp ZD, Grasemann B (1999) Himalayan inverted metamorphism constrained by oxygen isotope thermometry. Contrib Mineral Petrol 137:90-101

Vogel DE, Garlick GD (1970) Oxygen-isotope ratios in metamorphic eclogites. Contrib Mineral Petrol 28:183-191

Vry J, Brown PE, Valley JW, Morrison J (1988) Constraints on granulite genesis from carbon isotope compositions of cordierite and graphite. Nature 332:66-68

Wada H (1977) Isotopic studies of graphite in metamorphosed carbonate rocks of central Japan. Geochem J 11:183-197

Wada H (1978) Carbon isotopic study on graphite and carbonate in the Kamioka Mining District, Gifu Prefecture, Central Japan, in relation to the role of graphite in the pyrometasomatic ore deposition. Mineral Deposita 13:201-220

Wada H (1988) Microscale isotopic zoning in calcite and graphite crystals in marble. Nature 331:61-63

Wada H, Oana S (1975) Carbon and oxygen isotope studies of graphite bearing carbonates in the Kasuga area, Gifu Prefecture, central Japan. Geochem J 9:149-160

Wada H, Suzuki K (1983) Carbon isotopic thermometry calibrated by dolomite-calcite solvus temperatures. Geochim Cosmochim Acta 47:697-706

Wada H, Enami M, Yanagi T (1984) Isotopic studies of marbles in the Sanbagawa metamorphic terrain, central Shikoku, Japan. Geochem J 18:61-73

Waldron K, Lee MR, Parsons I (1994) The microstructures of perthitic alkali feldspars revealed by hydrofluoric acid etching. Contrib Mineral Petrol 116:360-364

Walker FDL (1990) Ion microprobe study of intragrain micropermeability in alkali feldspars. Contrib Mineral Petrol 106:124-128

Watson EB, Cherniak DJ (1997) Oxygen diffusion in zircon. Earth Planet Sci Letters 148:527-544

Weis PL (1980) Graphite skeleton crystals—A newly recognized morphology of crystalline carbon in metasedimentary rocks. Geology 8:296-297

Weis PL, Friedman I, Gleason JP (1981) The origin of epigenetic graphite: Evidence from isotopes. Geochim Cosmochim Acta 45:2325-2332

Wiechert U, Hoefs J (1995) An excimer laser-based micro analytical preparation technique for *in situ* oxygen isotope analysis of silicate and oxide minerals. Geochim Cosmochim Acta 59:4093-4101

Wright K, Freer R, Catlow CRA (1995) Oxygen diffusion in grossular and some geological implications. Am Mineral 80:1020-1025

Yapp CJ (1990) Oxygen isotopes in iron (III) oxides 2. Possible constraints on the depositional environment of a Precambrian quartz-hematite banded iron formation. Chem Geol 85:337-344

Young ED (1993) On the $^{18}O/^{16}O$ record of reaction progress in open and closed metamorphic systems. Earth Planet Sci Letters 117:147-167

Young ED, Fogel ML, Rumble D, Hoering TC (1998) Isotope ratio monitoring of O_2 for microanalysis of $^{18}O/^{16}O$ and $^{17}O/^{16}O$ in geological materials. Geochim Cosmochim Acta 62:3087-3094

Zhang Y, Stolper EM, Wasserburg GJ (1991) Diffusion of a multi-species component and its role in oxygen and water transport in silicates. Earth Planet Sci Letters 103:228-240

Zheng Y-F (1991) Calculation of oxygen isotope fractionation in metal oxides. Geochim Cosmochim Acta 55:2299-2307

Zheng Y-F (1992) Discussion on the use of δ–Δ diagram in interpreting stable isotope data. Eur J Mineral 4:635-643

Zheng Y-F (1993) Calculation of oxygen isotope fractionation in hydroxyl-bearing silicates. Earth Planet Sci Letters 120:247-263

Zheng Y-F (1993b) Oxygen isotope fractionation in SiO_2 and Al_2SiO_5 polymorphs: Effect of crystal structure. Eur J Mineral 5:651-658

Zheng Y-F (1993c) Calculation of oxygen isotope fractionation in anhydrous silicate minerals. Earth Planet Sci Letters 120:247-263

Zheng Y-F (1995) Oxygen isotope fractionation in magnetites: Structural effect and oxygen inheritance. Chem Geol 121:309-316

Zheng Y-F (1996) Oxygen isotope fractionations involving apatites: Application to paleotemperature determination. Chem Geol 127:177-187

Zheng Y-F, Fu B (1998) Estimation of oxygen diffusivity from anion porosity in minerals. Geochem J 32:71-89

Zheng Y-F, Simon K (1991) Oxygen isotope fractionation in hematite and magnetite: A theoretical calculation and application to geothermometry of metamorphic iron-formations. Eur J Mineral 3: 877-886

Zheng Y-F, Fu Bin YL, Xiao Y, Shuguang L (1998) Oxygen and hydrogen isotope geochemistry of ultrahigh-pressure eclogites from the Dabie Mountains and the Sulu terrane. Earth Planet Sci Letters 155:113-129

Zheng Y-F, Fu B, Yilin X, Yiliang L, Bing G (1999) Hydrogen and oxygen isotope evidence for fluid-rock interactions in the stages of pre- and post-UHP metamorphism in the Dabie Mountains. Lithos 46: 677-693

Zinner E, Ming T, Anders E (1989) Interstellar SiC in the Murchison and Murray meteorites: Isotopic composition of Ne, Xe, Si, C, and N. Geochim Cosmochim Acta 53:3273-3290

This page left blank.